JCI The Journal of Clinical Investigation

# IFNGR/STAT1 signaling in recipient hematopoietic antigen presenting cells suppresses graft-versus-host disease

Caisheng Lu, … , Suzanne Lentzsch, Markus Y. Mapara

*J Clin Invest.* 2022. https://doi.org/10.1172/JCI125986.

**Research** In-Press Preview **Immunology** **Transplantation**

## Graphical abstract

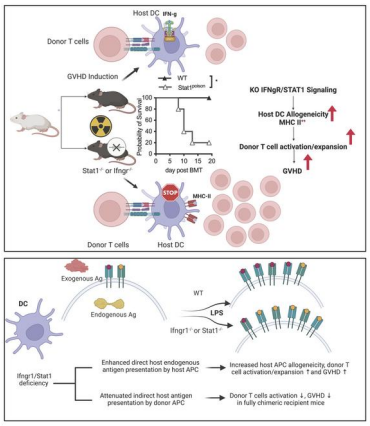


## Find the latest version:

https://jci.me/125986/pdf

# IFNGR/STAT1 Signaling in Recipient Hematopoietic Antigen Presenting Cells Suppresses Graft versus Host Disease

**Caisheng Lu[1+], Huihui Ma[1+], Liangsong Song[1], Hui Wang[1], Lily Wang[1], Shirong Li[2], Stephen Lagana[3], Antonia R. Sepulveda[3], Kasper Hoebe[4,5], Samuel S. Pan[6], Yong-Guang Yang[1], Suzanne Lentzsch[2], and Markus Y. Mapara*[1, 2]**

[1]Columbia Center for Translational Immunology. Columbia University, New York City, NY.
[2]Division of Hematology-Oncology, Columbia University, New York City, NY
[3]Department of Pathology, George Washington University, Washington, DC
[4]Department of Pediatrics, University of Cincinnati, OH
[5]Janssen Research & Development, Spring House, PA
[6]Herbert Irving Columbia Cancer Center, Cancer Biostatistics Shared Resource, New York, NY

**One Sentence Summary:** IFNGR/STAT1 signaling differentially regulates the presentation of endogenous versus exogenous antigens in hematopoietic APC.

[+] These authors should be considered joint 1st co-authors.

Word count: 10906

* To whom correspondence should be addressed:
Markus Y. Mapara, MD, PhD
Department of Medicine,
Division of Hematology-Oncology
Columbia Center for Translational Immunology
Columbia University, College of Physicians and Surgeons
Harkness Pavilion 11-31
New York, NY 10032
PHONE: 646-317-5689
email: mym2111@columbia.edu

## Abstract

Absence of Interferon-γ Receptor (IFNGR) or Signal Transducer and Activator of Transcription 1 (STAT1) signaling in donor cells have been shown to result in reduced acute GVHD induction. In this study, we unexpectedly observed increased activation and expansion of donor lymphocytes in both lymphohematopoietic organs and GVHD target tissues of IFNGR/STAT1-deficient recipient mice, leading to rapid mortality following the induction of GVHD. Lipopolysaccharide (LPS)-matured bone marrow-derived *Ifngr1*$^{-/-}$/*Stat1*$^{-/-}$ dendritic cells (BMDCs) were more potent allogeneic stimulators and expressed increased levels of MHC II and costimulatory molecules. Similar effects were observed in human APCs with knockdown of *Stat1* by CRISPR/Cas9 and treatment with a JAK1/2 inhibitor. Furthermore, we demonstrated that the absence of IFNGR/STAT1 signaling in hematopoietic APCs impaired the presentation of exogenous antigens while promoting the presentation of endogenous antigens. Thus, the indirect presentation of host antigens to donor lymphocytes was defective in IFNGR/STAT1-deficient donor-derived APCs in fully donor chimeric mice. The differential effects of IFNGR/STAT1 signaling on endogenous and exogenous antigen presentation could provide further insight into the roles of the IFN-γ/STAT1 signaling pathway in the pathogenesis of GVHD, organ rejection, and autoimmune diseases.

## Introduction

Interferon-gamma (IFN-γ) is a pleiotropic cytokine with a central role in host defense and immunopathology and is involved in both innate and adaptive immunity (1, 2). IFN-γ is the only type-II IFN family member produced by innate natural killer (NK), γδ-T, activated Th1, cytotoxic $CD8^+$, and professional antigen-presenting cells (APCs)(1-3). Acting synergistically with T cell receptor (TCR) stimulation as a prototypical Th1 cytokine, IFN-γ acts via the JAK1/STAT1 signaling pathway to drive the first wave of T-bet expression (4). T-bet serves as the master regulator of Th1 differentiation by promoting the expression of both IL-12-receptor-β2 and the production of IFN-γ (4). This effect renders cells responsive to IL-12/STAT4 and IFN-γ/STAT1 to maintain T-bet expression and Th1-specific cytokine production while inhibiting the differentiation and function of other Th subsets (4-6). In addition to its effects on Th differentiation, IFN-γ is known to promote macrophage activation (1, 2) and the expression of major histocompatibility complex (MHC) class II and IL-12, which further amplify IFN-γ production and Th1-mediated physiologic and pathologic immune responses (1, 3, 7-12). IFN-γ-signaling has been implicated in mediating tissue damage in the gastrointestinal tract (13, 14). Therefore, IFNGR signaling is emerging as an attractive target (15-17) for GVHD intervention, as corroborated by clinical results using the non-selective JAK1/2 inhibitor ruxolitinib and preclinical results with barcitinib (18, 19).

Conversely, evidence supports a protective role for IFN-γ in limiting inflammation-driven tissue damage. In particular, *Ifng*$^{-/-}$, *Ifngr1*$^{-/-}$ or *Stat1*$^{-/-}$ mice are significantly more susceptible to EAE (20-22), CIA(12), and acute GVHD induction (8, 10, 23-25). This inhibitory function of IFN-γ has been proposed to involve the induction of apoptosis of activated lymphocytes (26, 27), conversion of $CD4^+CD25^-$ T cells into $T_{reg}$ (28), and the induction of indoleamine 2,3-dioxygenase (IDO) and nitric oxide (NO) expression leading to tolerogenic dendritic cells (DCs)(1-3, 26). Furthermore, IFN-γ-induced PD-L1 expression negatively regulates T cell activation (29).

Here, we describe a novel modulatory role for IFN-γ/STAT1 in hematopoietic APC. We observed significantly enhanced GVHD induction and increased activation of alloreactive donor T cells by host IFNGR/STAT1-

deficient hematopoietic APC. The enhanced stimulatory capacity of IFNGR/STAT1-deficient APC was associated with the upregulation of MHC II expression and increased endogenous antigen presentation. Radiation bone marrow chimeric recipients with fully engrafted donor-derived IFNGR-deficient APCs had less indirect allostimulatory capacity resulting in attenuated activation of host-alloantigen specific donor lymphocytes from the delayed donor lymphocyte infusion (DLI) and development of GVHD. Our data suggest that IFNGR/STAT1 signaling in APCs functions as an immune rheostat to restrain auto-inflammation by suppressing endogenous antigen presentation under inflammatory conditions while enhancing responses against exogenous antigens.

## Results

*Absence of the IFNGR/STAT1 signaling in recipient mice leads to increased acute GVHD.* In the current study, we sought to investigate the effects of host STAT1 deficiency on the induction of acute GVHD. To this end, GVHD was induced in the fully MHC-mismatched BALB/c ($H2^d$) to 129 ($H2^b$) strain combination by injecting $5x10^6$ BALB/c T cell-depleted (TCD) BMCs plus $1x\ 10^7$ splenocytes into lethally irradiated *129.Stat1*$^{+/+}$ or *129.Stat1*$^{-/-}$ mice. The *129.Stat1*$^{-/-}$ recipients experienced significantly accelerated mortality (Figure 1A, median survival time (MST) 5 days vs. 7.5 days, log-rank test $p<0.0001$) and exacerbated morbidity measured by GVHD clinical scores (Supplementary Figure 1A). However, histopathological analysis of GVHD target organs obtained at day+4 showed no significant differences yet at this early time point between the wild-type and STAT1-deficient recipients (Supplementary Figure 1B). STAT1-deficient hosts receiving syngeneic BMCs and spleen cells did not exhibit increased morbidity or mortality, ruling out that enhanced sensitivity of STAT-deficient recipients to conditioning-induced toxicity accounted for the increased mortality. To investigate the inflammatory response following allogeneic BMT, we tested the early serum cytokine profiles of the recipient mice after lethal irradiation following BMT. Our data did not reveal increased serum levels of IL-1α, IL-6, TNF-α, RANTES, and MCP-1 on day+1, day+3 post-BMT in the Stat1$^{-/-}$ group. However, we observed significant increases in IL-12 and IL-4 on day+3 and/or day+4 post-BMT in the *Stat1*$^{-/-}$ recipient mice compared to their wild-type counterparts (Supplementary Figure 2), indicating dysregulation and skewing of the immune response. When recipient spleen cells were analyzed on day + 5 post-BMT by flow cytometry, we found increased expansion of donor T cells and elevated absolute numbers of activated donor $CD4^+$ T cells (Figure. 1B). The increase was associated with enhanced donor $CD4^+$ Th1 but comparable $CD8^+$ Tc1 differentiation in *Stat1*$^{-/-}$ recipients (Figure. 1C).

Using bioluminescence imaging (BLI), we tested *in vivo* expansion of donor cells and organ infiltration after the transfer of luciferase-expressing BALB/c splenocytes (BALB/c-luc) into lethally irradiated *B6.Stat1*-deficient or B6 wild-type recipients. B6 mice are more resistant to GVHD induction than the 129sv mice under the same transplantation conditioning, which allowed us to observe donor lymphocyte expansion after day+5 post-BMT.

Markedly enhanced expansion and organ infiltration of donor BALB/c-luc cells were detectable in the spleen, liver, lung, and gut of *B6.Stat1*$^{-/-}$ compared to B6 wild-type recipients (Figure 1D, Supplementary Figure 3A) on day + 6 post-BMT. We repeated our studies in a different STAT1-deficient strain (*B6.Stat1*$^{Poison}$ mice) to further validate our results. This mouse strain was generated by N-ethyl-N-nitrosourea (ENU)-induced mutagenesis, which affects the splice site upstream of exon 20 of the Stat1 gene to result in a truncated STAT1 protein(30). The phenotypes of STAT1$^{Poison}$ mice and 129.STAT1-deficient mice were consistent with our prior study (17) (Supplementary. Figure 4A and data not shown). In line with experiments performed with *129.Stat1*$^{-/-}$ mice, GVHD mortality significantly increased in *Stat1*$^{Poison}$ recipients (Supplementary Figure 4B). CD4$^{+}$ and CD8$^{+}$ T cell activation was also enhanced (Supplementary Figure 4C). Similar to the results by Burman et al. in *Ifngr1*$^{-/-}$ mice, we noted severe lung pathology (data not shown) but reduced damage to the GI tract in Stat1$^{Poison}$ recipients when the histopathological analysis was performed on day +8 post-BMT (Supplementary Figure 4D, 4E). These results confirm the differential role of IFNGR signaling in GVHD target organs (13).

We next delineated the contribution of IFN-γ signaling in recipient mice using the BALB/c→B6 model and the ability of IFN-γ signaling deficiency to recapitulate our STAT1 findings. Following the observation that GVHD-related mortality was significantly higher in Stat1$^{-/-}$ recipient mice than in the wild-type recipients, GVHD induction was accelerated considerably (MST 13 days in the Ifngr1$^{-/-}$ versus undefined in the wild-type group, Figure 1E) in the *B6.Ifngr1*$^{-/-}$ recipients following lethal irradiation (1,075 rad). This observation was consistent with the studies reported by Burman and colleagues (14). We observed enhanced activation and expansion of donor CD4$^{+}$ and CD8$^{+}$ T cells (Figure 1F) and significantly increased Th1 differentiation of donor CD4$^{+}$ lymphocytes (Figure 1G) in the spleens of the *Ifngr1*$^{-/-}$ recipient mice when tested on day +4 or +5 post-BMT. By using BLI analysis of recipients injected with BALB/c-luc spleen cells, we also observed significantly enhanced donor lymphocyte infiltration in the gut and spleen tested on day +4 post-BMT (Supplementary Figure 5B) in the *B6.Ifngr1*$^{-/-}$ recipients compared to B6 wild-type recipients. When studied on day +7 expansion, we observed a further increase in tissue infiltration (spleen, lung, and liver) by donor lymphocytes in

*B6.Ifngr1*$^{-/-}$ recipients. In contrast to *Stat1*$^{-/-}$ recipients, donor lymphocyte infiltration in the gut of *B6.Ifngr1*$^{-/-}$ recipients were comparable to their wild-type counterparts when assessed on day +7 (Figure 1H, Supplementary Figure 3B). These results suggest that lack of IFN-γ-signaling accelerated initial gut infiltration but did not result in further accumulation at later time points. Furthermore, our results indicate different roles in host STAT1 and IFNGR signaling regarding the recruitment of donor cells to the gut, which warrants further investigations.

*Contribution of hematopoietic versus non-hematopoietic IFNGR/STAT1 deficiency to the development of GVHD*. To determine the contribution of host hematopoietic vs. non-hematopoietic tissue to the promotion of GVHD, we created radiation bone marrow chimeric mice in which STAT1 deficiency was confined to the hematopoietic compartment and then induced GVHD via a second transplant. Thus, 129.*Stat1*$^{+/+}$ mice were lethally (1044rad) irradiated and reconstituted with either 129.*Stat1*$^{+/+}$ or *Stat1*$^{-/-}$ BMCs. The successful creation of radiation chimeras and the absence of STAT1 expression was confirmed by STAT1 staining in peripheral blood samples using flow cytometry (data not shown). On day +120 post-BMT, the mice were reconditioned (1,044 rad) and transplanted with 5x10$^6$ BMCs plus 5x10$^6$ spleen cells from BALB/c mice. As shown in Figure 2A, we observed accelerated GVHD mortality in BALB/c→(129.*Stat1*$^{-/-}$→129.*Stat1*$^{+/+}$) chimeric mice compared to BALB/c→ (129.*Stat1*$^{+/+}$→*Stat1*$^{+/+}$) chimeras (MST 6 days vs. 11 days, log-rank test p=0.02), suggesting that the absence of STAT1 in host hematopoietic tissue is sufficient to accelerate GVHD induction. Both *Stat1*$^{-/-}$ and the WT hosts receiving syngeneic BMCs and spleen cells did not exhibit mortality confirming the alloreactive responses are the driving force of acute GVHD induction in this model. In accordance with the increased mortality, donor T cell activation was significantly increased in BALB/c→ (129.Stat1$^{-/-}$ →129.*Stat1*$^{+/+}$*)* recipients tested on day +6 post-BMT (Figure 2B). To further confirm that the increased activation of donor lymphocytes was indeed triggered by STAT1-deficient host hematopoietic cells (and not by non-hematopoietic cells), we established similar chimeras using *B6.Stat1*$^{Poison}$ mice. *B6.Stat1*$^{Poison}$ mice or wild-type (*Stat1*$^{+/+}$) B6 mice (both CD45.2) were lethally (1075 rad) irradiated and reconstituted with B6.SJL

(CD45.1) BMCs before undergoing a second transplant for GVHD induction, as described above. In contrast to chimeric mice with exclusive hematopoietic STAT1 deficiency, donor T cell activation was not increased in the *B6.Stat1*$^{+/+}$→*Stat1*$^{Poison}$ chimeric recipient mice upon the induction of GVHD following re-transplant compared with that in the *B6.Stat1*$^{+/+}$→*Stat1*$^{+/+}$ chimeric mice (Figure 2C). These results suggest that the absence of STAT1 in non-hematopoietic host tissue is not critical to affecting the initial donor T cell activation, whereas STAT1 deficiency in the recipient hematopoietic cells is sufficient for enhanced donor T cell activation and subsequent morbidity and mortality.

Next, we determined the contribution of host hematopoietic vs. non-hematopoietic IFNGR deficiency in promoting GVHD. We created radiation bone marrow chimeric mice (B6.*Ifngr1*$^{-/-}$→B6.SJL) in which IFNGR deficiency was confined to the hematopoietic compartment, as described above. After reconditioning and the induction of GVHD [BALB/c→(B6.*Ifngr1*$^{-/-}$→B6.SJL]], we observed increased GVHD mortality (Figure. 2D) and enhanced expansion of infused donor BALB/c-luc lymphocytes in recipient chimeric mice lacking IFNGR on host hematopoietic cells, as tested by BLI (Figure 2E). Recipient non-hematopoietic IFNGR signaling had been reported to play an important role in reducing GVHD mortality (31). Our data also support this observation with MST 43 days (solid triangle in Figure 2D) in recipient mice with IFNGR deficiency restricted to the non-hematopoietic cells versus MST 15 days (solid circle in Figure 2F) in chimeric mice with intact IFNGR in both hematopoietic and non-hematopoietic compartments (Figure 2D, Figure 2F). Of note, compared to recipients deficient in IFNR expression only in non-hematopoietic tissue, GVHD-induced mortality was further enhanced when both hematopoietic and non-hematopoietic tissues (BALB/c→(*B6.Ifngr1*$^{-/-}$→B6.*Ifngr1*$^{-/-}$) lacked IFNGR (Figure 2F). These data suggest that the IFNGR/STAT1 signaling in the host hematopoietic compartments plays a vital role in reducing the activation of donor lymphocytes and the induction of acute GVHD in the MHC-mismatched BMT mouse model.

*Phenotypic and functional characteristics of IFNGR/STAT1-deficient APC.* Next, we investigated the impact of IFNGR/STAT1 deficiency on hematopoietic APC phenotype and function. To our surprise, MHC II surface

expression levels were significantly elevated on recipient IFNGR/STAT1-deficient APC compared to their wild-type counterparts as tested on day +1-3 post-BMT in the MHC-mismatched mouse GVHD model (Figure 3A, 3B). Our radiation chimera model further corroborated the results. Thus, surface expression of MHC II and CD86 was consistently higher on host splenic $CD11c^+$ cells in recipients lacking IFNGR only in the hematopoietic compartment (BALB/c→ (B6.*Ifngr1*$^{-/-}$ →B6.SJL)) compared to wildtype chimeric (BALB/c→ (B6 →B6.SJL)) controls (Figure 3C).

To further investigate the increased expression of MHC II and costimulatory molecules on APCs with IFNGR/STAT1 deficiency, we interrogated bone marrow-derived dendritic cells (BMDCs) isolated from either *Stat1*$^{+/+}$ or S*tat1*$^{-/-}$ mice for expression of MHC II, costimulatory molecules and their stimulatory capacity. LPS is one of the most commonly used reagents for BMDCs maturation and a key inflammatory factor driving GVHD induction after lethal conditioning (32). Consistent with the *in vivo* observations, STAT1-deficient BMDCs matured in the presence of LPS expressed increased MHC II and CD86 (Figure 3D) on the cell surface compared to their wild-type counterparts. In contrast, the co-inhibitory molecule PD-L1 expression was reduced upon LPS treatment (Figure 3D) in STAT1-deficient BMDC. Analysis of flow data from 6 separate *in vitro* experiments of LPS-maturated DC showed a significant increase in I-Ab expression on *Stat1*$^{-/-}$ DC compared to *Stat1*$^{+/+}$. Upregulation of CD86 and decrease of PD-L1 expression on *Stat1*$^{-/-}$ DC maturated with LPS was consistently observed in 4 and 3 experiments, respectively but did not reach statistical significance (Data not shown).

Given the increased MHC II and CD86 expression levels, matured STAT1-deficient DC would be expected to have increased allostimulatory capacity. To test this hypothesis, irradiated LPS-matured *Stat1*$^{+/+}$ or *Stat1*$^{-/-}$ BMDCs were co-cultured with fully MHC-mismatched (BALB/c) T cells at 1:5 T/DC ratios for five days. We were able to observe an enhanced proliferation of responder alloreactive T cells (Figures 3E, F) and a significantly increased proportion of activated ($CD44^+CD62L^{--}$) $CD4^+$ and $CD8^+$T cells (Figure 3G).

To determine the translational relevance of our above-described observations in mice, we tested the impact of deficient IFNGR/STAT1 signaling on the function and phenotype of human APCs. We used *Stat1* Clustered Regularly Interspaced Short Palindromic Repeats (CRISPR)-directed gene editing in freshly isolated Peripheral blood mononuclear cells (PBMCs). ATTO-positive cells were collected by Influx sorter, irradiated then used as stimulators to stimulate alloreactive human PBMCs in a mixed lymphocyte reaction (Supplementary Figure 6A). As expected, there was no proliferation (determined by CellTracer Violet low) and activation (determined by HLA-DR$^+$CD38$^+$ on CD4$^+$ or CD8$^+$T cells) of responder cells in the absence of stimulator cells. Control sgRNA transduced stimulator cells induced 40% proliferation and 10% activation of responder cells. In contrast, enhanced proliferation (60%) and activation (15%) of responder cells were observed when Stat1 sgRNA-treated stimulator cells were used (Supplementary Figure 6B). Next, we tested the effect of pharmacological JAK1 and JAK2 inhibition, which are upstream of STAT1 signaling. Ruxolitinib is a JAK1/JAK2 inhibitor that was recently FDA-approved for steroid-refractory GVHD. To delineate if JAK inhibition can mimic the data observed in gene-deficient murine APCs, additional studies were performed using human CD3/CD56 depleted PBMC treated with 5uM Ruxolitinib (Supplementary Figure 7A) as stimulator cells. In contrast to a previous report that Ruxolitinib inhibited DC activation and function (33), our data demonstrated that Ruxolitinib pre-treatment of CD3/CD56-depleted PBMCs leads to pronounced inhibition of PD-L1 expression while promoting HLA-DR and CD86 expression on CD11c$^+$ cells (Supplementary Figure 7B) associated with increased allo-stimulatory capacities in an MLR (Supplementary Figure 7C). The discrepancy to the published results may be partially due to our experimental system, which includes T lymphocyte and NK cell depletion. In addition, Heine et al. used plastic adherence to generate monocyte-derived DC, which may not necessarily deplete lymphocytes. Ruxolitinib is well known for its inhibition of T and NK cell functions. Its influence on the purified APC population, including DCs, warrants further investigation.

*Effect of IFNGR/STAT1 signaling on endogenous and exogenous antigen presentation.* The activation of donor CD4$^+$ T cells requires the cognate interaction of their TCR with allopeptides presented within the context of

MHC II molecules by the host or donor APCs (31, 34). Alloreactive donor $CD4^+$ T cells can recognize host alloantigens in the context of MHC II via the direct or indirect pathway (34). In the direct pathway, donor T cells recognize host allopeptides in the context of intact host MHC molecules on the surface of recipient APCs. In the indirect pathway, donor T cells recognize host-derived allopeptides taken up, processed, and presented by MHC II on donor APCs. Therefore, we assessed the effect of IFNGR/STAT1 signaling on the presentation of exogenous versus endogenous peptides in the context of MHC II.

Given the increased MHC II expression observed on host hematopoietic APCs lacking IFNGR or STAT1 during the induction of GVHD, we assessed the association between enhanced MHC II expression and the increased presentation of host-derived endogenous peptides. The semiallogeneic B6.SJL→$CB6F_1$ GVHR model without conditioning allowed us to identify self-peptide presentation by host APCs and subsequent antigen-specific donor T cell responsiveness. CB6.F1 mice express BALB/c-derived MHC class II Eα self-peptide (peptide 52-68), which is presented by $I\text{-}A^b$ molecules, and this $E\alpha/I\text{-}A^b$ complex is recognized by both the Y-Ae antibody and the TEa TCR (31, 35). For this experiment, $2.5\text{-}3x10^7$ splenocytes from B6.SJL mice and $5x10^6$ TCD BMCs from B6 mice were injected into either wild-type or *Ifngr1*$^{-/-}$ CB6F1 mice without irradiation. By the above data, the absence of IFNGR expression on $CB6F_1$ recipient APCs promoted the expression of MHC class II ($I\text{-}A^b$) on host $CD11c^+$ cells compared to CB6F1 wild-type recipients following the administration of semiallogeneic B6 spleen cells tested on day +1 post-transplantation. Y-Ae binding on host $CD11c^+$ cells from CB6F1 *Ifngr1*$^{-/-}$ recipients was significantly increased (Figure 4A).

Next, we confirmed that the enhanced Y-Ae expression on host APCs in *Ifngr1*$^{-/-}$ CB6F1 mice elicited an enhanced Eα52-68 peptide-specific donor T cell response. To this end, TEa-TCR-Tg $CD4^+$ were co-administered to CB6F1*Ifngr1*$^{-/-}$ or wild-type CB6F1. As hypothesized, we observed markedly increased donor Tea-$TCR^+$ $CD4^+$ T cell activation (Supplementary Figure 8A), Th1 differentiation (Supplementary Figure 8B), reduced $T_{reg}$ differentiation (Supplementary Figure 8C), and increased proliferation as determined by BrdU incorporation (Supplementary Figure 8D) in CB6F1.*Ifngr1*$^{-/-}$ recipients. These findings suggested that the absence of

IFNGR/STAT1 signaling in recipient APCs enhanced host MHC II-dependent presentation of Eα52-68 and promoted recognition by donor TEa-TCR$^{+}$ CD4$^{+}$ T cells.

The absence of IFNGR or STAT1 in macrophages or dendritic cells has been reported to result in defective antigen presentation for intracellular pathogens (36-39). To assess the effect of IFNGR/STAT1 signaling more clearly on the presentation of exogenous antigens, we used ovalbumin (OVA) as an additional model antigen system. We studied the proliferation/activation of responder CD4$^{+}$ OT-II cells as a readout for effective antigen presentation in APCs in the presence or absence of IFNGR/STAT1-signaling. As expected, OT-II cells did not proliferate when co-cultured with BMDCs maturated by LPS without exogenous OVA protein (Figure 4C, red line). At the same time, the ability of IFNGR- or STAT1-deficient BMDCs incubated with exogenous full-length OVA protein to promote OT-II proliferation was severely compromised (Figure 4B upper panel, and Figure 4C blue line). In contrast, OT-II proliferation was not diminished when stimulated with IFNGR-deficient BMDCs that had been loaded with $OVA_{323-339}$ peptide (Figure 4B lower panel), which does not require intracellular antigen processing and presentation but depends on surface MHC II expression, indicating that direct loading of the peptide onto the MHC II peptide-binding groove was not impaired.

We next utilized transgenic act-mOVA mice that exhibit constitutive membrane-associated OVA expression in all tissues under the control of the actin promoter as a model of the endogenous self-peptide presentation via MHC II. When these LPS-matured, mOVA-expressing and STAT1-deficient BMDCs were used as stimulators, we observed markedly increased OT-II cell proliferation in response to *Stat1*$^{-/-}$ act-mOVA-expressing BMDCs compared to wild-type act-mOVA-expressing BMDCs (Figure 4D upper panel), suggesting that the absence of STAT1 signaling promoted the MHC II-dependent presentation of self-peptides of ovalbumin. In contrast, there was no OT-II cell proliferation in response to both wild-type and STAT1$^{-/-}$ BMDCs confirming the OT-II proliferation was ovalbumin specific (Figure 4D low panel). The activation and Th1 differentiation of OT-II cells was significantly enhanced on day +3 after injection into lethally irradiated act-mOVA STAT1-deficient mice compared to STAT1-wildtype act-mOVA mice (Figure 4E). In summary, these results indicate that the absence

of IFNGR/STAT1 signaling impairs the processing and presentation of exogenous antigen by MHC II in hematopoietic APCs while promoting the presentation of endogenous self-peptides.

*Impact of IFNGR/STAT1 signaling on direct and indirect antigen presentation.* Next, we studied the role of IFNGR signaling in a P →F1 (B6.SJL[$H2^b$] →CB6F1 [$H2^{bxd}$]) model without host irradiation. Under this scenario I-Ab molecule in CB6F1 mice presents multiple endogenous parental BALB/c H-$2^d$ derived peptides to alloresponsive parental SPCs. Administration of $2.5x10^7$ SPCs from B6 mice to CB6F1 $Ifngr1^{-/-}$ recipient mice led to significantly increased GVH-induced mortality (Figure 5A) and GVHD target tissue pathology when studied on day +30 post-BMT (Supplementary Figure 9). Analysis of peripheral blood, spleen, and lymph nodes on day +7 post-transplant demonstrated increased expansion and activation of donor $CD4^+$ and $CD8^+$ T cells (Figure 5B and data not shown). Furthermore, enhanced Th1 and Th17 differentiation of donor $CD4^+$ lymphocytes were observed in IFNGR-deficient CB6F1 recipients, whereas $T_{reg}$ differentiation was significantly reduced (Figure 5C).

Based on the observed impaired presentation of exogenous OVA (Figure 4 B-D) by STAT1-deficient APC *in vitro* and *in vivo*, we postulated that the absence of IFNGR/STAT1 signaling in donor APCs would impair host antigen presentation via the indirect pathway. To test this hypothesis, we generated bone marrow chimeric mice by reconstituting lethally irradiated BALB/c mice with *B6.Stat1*$^{+/+}$ or *B6.Stat1*$^{-/-}$ T cell-depleted bone marrow cells. Full donor cell hematopoietic engraftment of recipient BALB/c mice was confirmed on day +18 post-BMT (Data not shown). In these chimeric animals, the host (BALB/c) tissue-derived Eα52-68 peptide can only be presented by donor APC, i.e., B6, through the indirect pathway via I-Ab. To this end, we first assessed Y-Ae expression on donor $CD11c^+$ I-$Ab^+$ cells. Figure 5D and 5E show significantly more Y-$Ae^+$ $CD11c^+$ cells in the wild-type B6→BALB/c than in the *B6.Stat1*$^{-/-}$→BALB/c chimeric mice on day +18 after the first transplant, demonstrating defective indirect Eα52-68 peptide presentation of I-Ab by *Stat1*$^{-/-}$ B6 donor APCs. These results were further confirmed by transferring Eα52-68 peptide-specific TEa-TCR-Tg donor CD4 T cells into *B6.Stat1*$^{-/-}$→BALB/c or B6→BALB/c chimeras three weeks after the initial transplant. In this model, the transferred TEa-

$TCR^+CD4^+$ T cells can only respond to the Eα52-68 peptide presented by $I\text{-}Ab^+$ hematopoietic APCs. We observed significantly reduced *in vivo* proliferation (Figure 5F, 5G), decreased activation (Figure 5H), and Th1 differentiation (Figure 5I) of TEa-TCR-Tg $CD4^+$T cells in B6.Stat1$^{-/-}$→BALB chimeric mice compared to *B6.Stat1*$^{+/+}$→BALB/c chimeras. Accordingly, TEa-TCRTg DLI-induced GVHD was reduced in Stat1$^{-/-}$ chimeric mice (Figure 5J) compared to wild-type chimeras. In our current model, we cannot clearly distinguish whether the reduced activation and proliferation of TEa-TCR CD4+ T cells are due to reduced processing and presentation or secondary to lower expression of MHC II leading to subsequently reduced presentation of Eα52-68 peptide or both.

*Absence of STAT1 leads to dysregulation of antigen processing and master genes controlling MHC II expression.* Given the imbalanced antigen presentation of exogenous OVA versus endogenous OVA and the altered MHC II expression levels in IFNGR/STAT1-deficient mature APCs, we explored potential mechanisms underlying this effect. The transmembrane α- and β-chains of MHC II are assembled in the endoplasmic reticulum, where they associate with the invariant chain (Ii, CD74) (40). The resulting Ii-MHC II complex is transported to a late endosomal compartment termed the MHC II compartment (MIIC), where Ii is digested by cathepsin S (CTSS), leaving only a small fragment called CLIP. This fragment blocks peptide-binding until H2-DM interacts with MHC II, which releases CLIP and permits the binding of a specific peptide derived from exogenous proteins degraded in the endosomal pathway. Figure 6A and 6B show that CD74 expression was comparably high in both wild-type and STAT1$^{-/-}$ immature BMDCs. As expected, LPS stimulation reduced CD74 expression as BMDCs maturated. It was noted that the Mean Fluorescence Intensity (MFI) of CD74 remained higher in both Ifngr1$^{-/-}$ and Stat1$^{-/-}$ BMDCs than in wild-type BMDCs, suggesting a defect in invariant chain release from MHC II. Moreover, CTSS is critical for degrading the Ii chain bound to MHC II before peptide exchange can occur (41). Consistently, the Ctss mRNA expression was significantly reduced in both *Ifngr1*$^{-/-}$ and *Stat1*$^{-/-}$ BMDCs compared to wild-type BMDCs after LPS stimulation (Figure 6C). Furthermore, as mentioned above, H2-DM is critical in facilitating peptide exchange and displacing the Ii chain with endosome-derived peptides (42, 43). After 4hr of

LPS stimulation, H2-DMb1 mRNA expression levels were significantly lower in *Ifngr1*$^{-/-}$ and *Stat1*$^{-/-}$ BMDCs compared to their wild-type counterparts (Figure 6C). These data suggest that peptide exchange in the MIIC may be defective in *Ifngr1*$^{-/-}$ and *Stat1*$^{-/-}$ BMDCs. Furthermore, post-translational regulation of MHC II expression by ubiquitination is another critical process in controlling antigen presentation. Usually, the ubiquitination process is suppressed in LPS-matured DCs (44, 45). MARCH1, an E3 ubiquitin ligase constitutively expressed by resting B cells and immature DCs, mediates the ubiquitination of internalized peptide-MHC II complexes at the plasma membrane and early endosomes targeting these complexes for lysosomal degradation (40, 45, 46). Under normal conditions, the maturation of DCs rapidly terminates MARCH1 expression to spare p-MHC II complexes from the lysosomal degradation (45).). March1 mRNA expression (Figure 6D) decreased after LPS maturation, and there was a further reduction in both *Ifngr1*$^{-/-}$ and *STAT1*$^{Poison}$ BMDCs compared to wild-type BMDCs upon LPS maturation. These data suggest reduced p-MHC II complex degradation and turnover in APCs with IFNGR/STAT1 deficiency. In addition to CTSS, many other lysosomal enzymes are critical for the degradation of phagocytosed proteins (47). We observed a slightly reduced staining with LysoTracker of IFNGR/STAT1-deficient APC at baseline in immature BMDC. However, upon LPS maturation, STAT1 or IFNGR-deficient APC failed to show any increase in Lysotracker staining (Figure 6E) compared to wildtype BMDC, suggesting impaired lysosomal activity in STAT1 or IFNGR-deficient APC may mitigate the degradation of phagocytosed proteins. As previously reported by others, autophagy delivers cytoplasmic constituents to the autophagosome (48). Further, it plays a critical role in MHC II antigen presentation for cytoplasmic constituents and self-peptides (48). The defective lysosome function in IFNGR or STAT-deficient BMDCs prompted us to assess autophagy markers. LC3B expression was studied in *Ifngr1*$^{-/-}$ and *Stat1*$^{-/-}$ BMDCs and suggested increased autophagy (Figure 6F). In summary, these data indicate that the absence of STAT1 signaling leads to attenuated lysosomal degradation, defective peptide exchange, and thus impaired exogenous antigen presentation but also provides evidence for the increased autophagic activity that might account for the increased endogenous antigen presentation through MHC II. These descriptive results indicate that the absence of IFNGR/STAT1-signaling in DCs affects multiple antigenic peptide processing and presentation levels.

## Discussion

In our current study, we have made several novel observations that may help to understand how IFNGR/STAT1 signaling regulates the development of GVHD through host vs. donor hematopoietic APC (Supplemetary Figure10). Our main finding suggests that the absence of IFNGR or STAT1 signaling in recipient hematopoietic APC promotes GVHD by enhancing host APC stimulatory capacity. We believe that our previously published (17) and current results provide the following framework of the role of IFN-γ in GVHD: 1) IFNGR/STAT1 signaling differentially controls GVHD based on the target cell: 1) IFNGR/STAT1 signaling promotes GVHD by inhibiting donor $T_{reg}$ cells while promoting Th1 type responses. 2) Lack of IFNGR/STAT1 signaling in host recipient APC results in pronounced activation of donor lymphocytes by the enhanced direct allostimulatory capacity of the APC. 3) IFNGR/STAT1 signaling in donor-derived APC assists the indirect presentation of host alloantigen to donor T cells to promote GVHD. 4) Finally, IFNGR signaling in hematopoietic APCs functions as a molecular switch in balancing exogenous versus endogenous antigen presentation.

Studies from several investigators support our main observation that the IFNGR-STAT1 axis has an inhibitory role in hematopoietic APC. Thus, Thome et al. reported that STAT1 was required for the function of tolerogenic DC using an EAE mode (49). Similarly, Vogel et al. (50) recently demonstrated that JAK1 inhibitor filgotinib-treated or JAK1-deficient APC had enhanced stimulatory capacity also in an EAE model. Interestingly, treatment with Filgotinib, a selective JAK1 inhibitor, promoted the expression of MHC II and costimulatory molecules on APC. In contrast, the absence of JAK1 did not have this effect despite promoting the stimulatory function. Furthermore, Vogel et al. showed that DC-intrinsic IFN-γ-dependent JAK1-STAT1 signaling promoted the expression of PD-L1, leading to enhanced Treg production and peripheral tolerization in the EAE model. Although we also observed IFNGR/STAT1-dependent regulation of PD-L1 expression on hematopoietic APC, we did not observe changes in Tregs in our recipients, arguing against a direct Treg-dependent effect in our model.

Our results further contribute to the existing evidence demonstrating differential regulation of GVHD (8-10) by IFN-γ. *Ifngr1*$^{-/-}$ or *Stat1*$^{-/-}$ donor T cells are severely impaired in their ability to induce GVHD across major and minor histocompatibility disparities with a concomitant reduction in Th1 differentiation and increased $T_{reg}$ generation, suggesting the IFN-γ signal pathway in donor lymphocytes is critical in CD4- and CD8-mediated GVHD (14, 15, 51, 52). Neutralization of IFN-γ or administration of IFN-γ-deficient donor T cells in the B6 to B6D2F1 model under non-irradiated conditions resulted in delayed GVHD mortality that was associated with impaired CTL function, reduced elimination of recipient cells, enhanced Th2 differentiation, and chronic GVHD-like features when compared to recipients of wild type grafts (53). In contrast, administration of recombinant IFN-γ protected recipient mice from GVHD and was associated with reduced donor T cell activation (54).

Several studies have reported that the absence of IFNGR in recipient mice accelerates and enhances GVHD mortality and is associated with severe lung damage (14) and bone marrow failure (25). Burman et al. (14) demonstrated that the detrimental effects of IFN-γ on GVHD induction are mediated through donor T cells, while the protective effects of IFN-γ are mediated through host tissue. In another mHA-mismatched MHC-matched BMT study using *Ifngr1*$^{-/-}$ as recipients, bone marrow failure occurs due to the exposure of donor hematopoietic cells to excessive amounts of IFN-γ accumulating in *Ifngr1*$^{-/-}$ recipients (25). Furthermore, Takashima et al. reported attenuated apoptosis in intestinal epithelial cells and crypt stem cells in the absence of IFN-γ signaling (13). Further studies indicate a complex regulation of the signaling molecules that regulate interferon signaling and Th1 response during GVHD. The absence of MiR-146 in recipients promoted GVHD, which was associated with increased JAKs/STATs signaling and involved regulation of MHC II (55). MiR-146 has been reported to act as a negative feedback controller of LPS/TLR-4 signaling (56). These findings suggest that miR-146 deficiency leads to a much broader inflammatory response than the activation of STAT1 alone. Paradoxically, deficiency of T-bet in recipient mice attenuated GVHD in MHC-mismatched models (57). This paradoxical role of T-bet and IFNGR/STAT1 has also been observed in other disease models (12, 58). Interestingly, we found increased levels of IL-12p70 in our STAT1-deficient recipients at day +3 post-BMT (Supplementary Figure 2). In contrast,

recipient mice with T-bet deficiency had reduced IL-12 and IFNγ production (57, 59). Furthermore, T-bet-deficient APC mice are impaired in their ability to induce Th1 differentiation and antigen-specific T cell activation (60), which may explain the differential GVHD induction in IFNGR/STAT1 vs. T-bet-deficient recipient mice.

Our results support the notion that IFNGR/STAT1 signaling in host hematopoietic APCs may be an early negative regulator of host endogenous antigen presentation and MHC II expression and thus suppress the activation of donor lymphocytes. We postulate that IFN-γ suppresses host-derived peptide/MHC II complex presentation on host hematopoietic APCs at early time points post-transplant, leading to reduced donor TCR engagement. Our findings are in potential discord with the results by Delisle, who showed reduced MHC II expression on day +8 following induction of mHA-mismatched GVHD (25). Several reasons could account for these apparent discrepancies, the most crucial difference being that Delisle et al. studied MHC II expression in GVHD target organs on non-hematopoietic cells and not in BMDC. We have preliminary observations that MHC II expression is reduced in epithelial cells of GVHD organs (e.g., intestinal epithelial cells, data not shown). Furthermore, based on our studies, the time point of studying MHC II expression will be crucial. We argue that priming of donor lymphocyte activation should occur before day 3-5 post-BMT and that hematopoietic-APC will be quickly eliminated given the intense lymphohematopoietic graft versus host (LHGVH) response of activated donor T cells.

Notably, our data demonstrate that IFNGR/STAT1 signaling in APC will have differential effects on GVHD development depending on the host or donor origin of the APC: Absence of IFNGR/STAT1-signaling promotes direct antigen presentation in host APC and will therefore lead to increased GVHD. Conversely, the lack of IFNGR/STAT1-signaling will mitigate GVHD by reducing the indirect presentation of host antigens by donor APC to donor T cells. Capitini and colleagues reported that fully-chimeric mice generated with $STAT1^{-/-}$ BM prevent GVHD induction by delayed allogeneic wild-type donor lymphocyte infusion. Their explanation for this attenuated GVHD was that STAT1-deficient $CD9^{-}$ $SiglecH^{hi}$ donor plasmacytoid dendritic cells (pDC) were tolerogenic and crucial for the reduced induction of GVHD (61) through increased IL-10 and reduced IL-12 and

IFN-α production. Using fully-chimeric mice generated with *Ifngr1*$^{-/-}$ BM, we observed reduced GVHD by delayed allogeneic wild-type donor lymphocyte infusion. As stated above, our results suggest that impaired indirect host antigen presentation may be an additional mechanism of the GVHD-mitigating effects of IFNGR/STAT1 deficient APC, resulting in attenuated activation of host peptide-specific donor T lymphocytes and consequently suppressed GVHD induction.

Non-selective JAK inhibitors like Ruxolitinib have recently been approved for steroid-refractory GVHD. We posit that the ruxolitinib-dependent anti-GVHD effects are not only mediated by direct inhibition of donor T cell responses and IFNγ-mediated cytopathic effects in the GVHD target tissue but also involve mitigation of indirect presentation of host antigens by donor APC. However, we would caution that the presence of host APC JAK inhibitors may worsen the development of GVHD. Our data here provide evidence that defective IFN-γ/STAT1 signaling may increase endogenous antigen presentation with the potential for enhancing autoimmunity and impaired protective immunity against exogenous pathogens. Consistent with this implication, Shao et al. (61) recently reported that STAT1-deficient hosts are more susceptible to the induction of cGVHD with enhanced anti-dsDNA autoantibody responses, increased proteinuria, and mortality. Furthermore, our results may allow us to test whether engineering the IFNGR/JAK1/STAT1-signaling pathway in APCs could be of value to achieving a more efficient presentation of endogenous tumor-associated peptides to $CD4^+$ T cells and potentially enhance tumor responses. In summary, our data document a regulatory role of IFN-γ/STAT1 signaling in hematopoietic APCs that modulates GVHD induction by suppressing direct antigen presentation of host APC while promoting indirect antigen presentation through donor APC.

## Methods

*Mice.*

Wild-type 129S6/SvEv mice [*129.Stat1*$^{+/+}$(H2$^{b}$)], C57BL/6 [(H2$^{b}$), B6], B6.SJL-Ptprca (B6.SJL, H2$^{b}$), BALB/c (H2$^{d}$), CB6F1, B6.Act-mOVA, B6.IFN-γ-Receptor1 (*B6.Ifngr1*$^{-/-}$), BALB/cByJ. *Ifngr1*$^{-/-}$, *B6.Stat1*$^{-/-}$, OTII, C.FVB-Tg (CAG-luc-GFP, BALB/c-Luc), and B6.TEa-TCR-Tg mice (B6.TEa) were purchased from Jackson Laboratories or Taconic. Act-mOVA-*Stat1*$^{-/-}$ (OVA-*Stat1*$^{-/-}$) and Act-mOVA-*Ifngr1*$^{-/-}$ (OVA-*Ifngr1* $^{-/-}$) were created by breeding B6.Act-mOVA with *B6.Stat1*$^{-/-}$ and *B6.Ifngr1*$^{-/-}$ mice, respectively. CB6F1.*Ifngr1*$^{-/-}$ mice were generated by breeding *B6.Ifngr1*$^{-/-}$ with BALB/cByJ.*Ifngr1*$^{-/-}$. *B6.Stat1*$^{Poison}$ (*Stat1*$^{Poison}$) mice (ENU mutagenesis-derived mutant with complete loss of STAT1 function) were generated by K. Hoebe (Cincinnati Children's Hospital Medical Center, Cincinnati, OH) (30). All mice were used between 8-12 weeks of age, housed in autoclaved microisolator environments, and provided with sterile water and irradiated food ad libitum. All manipulations were performed in a laminar flow hood.

*BMT and induction of GVHD.*

Mice were transplanted as described previously(51). Mice received total body irradiation (TBI) as follows: B6-background, 1075cGy; 129-SvEv background, 1044cGy; BALB/c, 800cGy. Lethally irradiated mice were reconstituted with 5x10$^{6}$ T cell-depleted allogeneic or syngeneic bone marrow cells (BMCs). T cell depletion (TCD) was performed using CD90.2 microbeads (Miltenyi Biotec). GVHD was induced by co-injecting allogeneic spleen cells or selected T cell populations, as described below. For B6 →CB6F1 (P→F1) graft-versus-host reaction (GVHR) model, non-irradiated F1 recipients (WT or *Ifngr1*$^{-/-}$) received 5x10$^{6}$ BMCs and 25 x10$^{6}$ splenocytes from B6.SJL or 3 x10$^{6}$ TEa cells. Pan T cells or naïve CD4$^{+}$ T cells were purified from splenocytes by using the Pan T Isolation Kit II or CD4$^{+}$ Isolation Kit (Miltenyi Biotec) according to the manufacturer's recommendations (purity ≥95%) and in some experiments labeled with 5 μM CFSE (Invitrogen) to assess *in vitro* and *in vivo* proliferation according to manufacturer's recommendations. For *in vivo* ovalbumin (OVA) pulse experiments, mice were I.P. injected with 100ug/mouse OVA (Ovalbumin EndoFit™, InvivoGen) emulsified in

Incomplete Freund adjuvant (IFA, InvivoGen) one hour before irradiation. For survival experiments, the degree of systemic GVHD was measured with a validated clinic scoring system (51). To avoid bias from cage-related effects, animals in different groups were randomized between cages.

*Creation of bone marrow radiation chimeras and DLI.*

For 129SvEv-background *Stat1*$^{-/-}$ chimeras (*Stat1*$^{-/-}$→*Stat1*$^{-/-}$), lethally irradiated 129.*Stat1*$^{+/+}$ mice were infused with 5x10$^6$ TCD BMCs from either 129.*Stat1*$^{-/-}$ or 129.*Stat1*$^{+/+}$ donors. The absence of STAT1 in host hematopoietic cells was confirmed by testing intracellular STAT1 expression in PBMCs two months post-BMT (data not shown). For *B6.Stat1*$^{Poison}$ chimeras (B6.SJL$^{-}$→ *B6.Stat1*$^{Poison}$) in which STAT1 deficiency was confined to the non-hematopoietic organs, lethally irradiated B6.*Stat1*$^{Poison}$ or B6 WT mice received 5x10$^6$ TCD BMCs from B6.SJL mice. For *B6.Ifngr1*$^{-/-}$ to WT chimeras (*B6.Ifngr1*$^{-/-}$→B6.SJL) in which IFNGR1 deficiency was confined to hematopoietic cells, lethally irradiated B6.SJL WT mice received 5x10$^6$ TCD BMCs from *B6. Ifngr1*$^{-/-}$ mice; B6.SJL→*B6. Ifngr1*$^{-/-}$ chimeras in which IFNGR deficiency was confined to the non-hematopoietic organs, lethally irradiated *B6.Ifngr1*$^{-/-}$ mice received 5x10$^6$ TCD BMCs from B6. SJL. Subsequently, these mice were reconditioned with TBI and injected with 5x10$^6$ BMCs and 5x10$^6$ spleen cells from BALB/c or BALB/c-Luc mice for induction of GVHD. For Stat1$^{-/-}$ or WT to BALB/c chimeras, lethally irradiated BALB/c mice received *Stat1*$^{-/-}$ or WT TCD BMCs. Examination for chimerism was performed on day+18, and GVHD was induced by DLI transferring 3x10$^6$ CellTrace™ Violet labeled TEa cells at day+20 post-BMT.

*BMDCs generation, phenotypic and functional assays.*

Bone marrow-derived dendritic cells (BMDCs) were generated from murine BMCs cultured in a medium containing murine GM-CSF (20 ng/ml, Peprotech). On days 6-7, non-adherent cells were harvested, and CD11c$^+$ DCs were purified with CD11c$^+$ microbeads (purity>90%, Miltenyi Biotec) and matured with LPS (100 ng/ml) for 4-48 h. For gene expression assay, cells were harvested at 4hr after LPS; For the phenotypic assay, cells were harvested at 24 h or 48 h; For *in vitro* antigen presentation experiments, BMDCs were pulsed with OVA 100ng/ml or OVA 323-339 for 2 h, then followed by LPS stimulation overnight. Suspension cells were fixed with 0.5%

paraformaldehyde (PFA) and then cocultured with CFSE-OTII cells at a 1/5 ratio for 4-5 days. For mixed lymphocyte reaction assay, LPS-matured BMDCs were irradiated with 3,000 cGy and used as stimulator cells, followed by co-culture with allo-responder cells labeled with 5uM CFSE, and cell proliferation was detected by CFSE dilution using flow cytometry. Alternatively, the proliferation of responder cells was measured by $^{3}$H-thymidine incorporation assay (1 uCi/well[0.037MBq] during the last 18 hours of culture and then harvested and counted using a Topcount Microplate (Packard), presented as counts per minute (CPM). All experiments were performed in triplicate.

*CRISPR/Cas9-mediated Stat1 genomic targeting.*

2.5nM Stat1crRNA (IDT, predesigned crRNA) or negative control crRNA (IDT)+ tracrRNA-ATTO (IDT) were incubated together with 0.15ug/ul TrueCut™ Cas9 Protein v2 (Invitrogen, A36498) for 10 min at room temperature to form the CRISPR-CAS9-gRNA RNP complex. Freshly isolated PBMCs ($5x10^{6}$) were transfected with an RNP mixture by Lipofectamine CRISPRMAX Cas9 Transfection kit (Invitrogen, CMAX00003) following the kit instruction. Twenty-four hours after transfection, replace the medium with 1 ml fresh culture medium (10% human AB serum AIM-V) for each well of a 24-well. Three days after transfection, the ATTO $550^{+}$ cells were sorted and irradiated at 3000cGy. The irradiated cells were cocultured with 5uM CFSE labeled allo human PBMCs at a 1:1 ratio in 96 round bottom plates. After 4 days of culture, the cells were harvested for flow cytometry analysis. All experiments were performed in triplicate. The knockdown effects within the PBMC bulk population were confirmed by Western blot.

*JAK inhibitor Ruxolitinib (Rux) treatment.*

Human PBMCs were depleted with CD3 and CD56 microbeads (Miltenyi Biotec). CD3/CD56 depleted PBMCs were treated with 5uM Rux (Selleck Chemicals) for 4hrs and followed with 100ug/ml LPS stimulation for additional 48hrs. After stimulation, the cells were irradiated with 3000cGy. To analyze allo-stimulatory capacity, irradiated cells were cocultured with 5uM CellTrace-Violet labeled allo-human PBMCs at a 1:1 ratio for 4 days; CD25 expression and Violet dilution on $CD4^{+}$ and $CD8^{+}$ T cells were studied by FCM.

*Flow cytometric analysis (FCM).*

Single cells were prepared and analyzed using FCM with LSRII or CantoII flow cytometer (BD Biosciences) and Flowjo or FCSExpress software. Cells were stained for 30 min at 4°C. For intracellular staining, $1x10^6$ cells were stimulated with PMA (50 ng/ml) and ionomycin (1μg/ml) in the presence of monensin (10μg/ml) in 1 ml of complete medium for 4 hours at 37°C in 5% $CO_2$. The cells were stained with surface antibodies for 30 min at 4°C, fixed/permeabilized, and then followed with intracellular staining. The antibodies used for these studies are shown in Supplementary Table I.

*In vivo labeling of mouse cells with Bromodeoxyuridine (BrdU).*

Splenocytes were isolated 24 hours after i.p. injection with 200 μl (2mg) of 10mg/ml BrdU solution (BD Biosciences). Then, SPCs were stained with FITC-labeled anti-BrdU and other markers.

*Lysotracker labeling.*

Treated or untreated BMDCs were loaded with 10-75 nM Lysotracker Deep Red (LDR, Invitrogen) according to the manufacturer's instructions by incubating the cells with dye for 30 min at 37°C, followed by washing and analysis by flow cytometry.

*Histology.*

For histopathological analysis of GVH target tissues, samples were collected and fixed in 10% Formalin. Samples were embedded in paraffin, cut into 5-um-thick sections, and stained with hematoxylin and eosin for histological examination.

*Bioluminescence imaging (BLI).*

T cell expansion was analyzed based on luciferase signal intensity. Briefly, the mice were I.P. injected with luciferin (200 ng/g body weight) and euthanized 7 min later. The organs were then imaged using a Xenogen IVIS 100 (Perkin Elmer) for 30 seconds. The imaging data were analyzed with the Living Image Software (Perkin Elmer) and presented as photons per second.

*Real-time quantitative PCR analysis.*

Total RNA was isolated with TRIzol reagent (Invitrogen), and cDNA was generated with the Superscript III RT kit (Invitrogen). PCR was carried out with SYBR Green PCR master mix (Applied Biosystems). The following primers sets were used: *Ctss, H2Dmb1,* and *March1* primers, obtained from QIAGEN, and *β-actin* sense 5′ GAA ATC GTG CGT GAC ATC AAA G 3′ and antisense 5′ TGT AGT TTC ATG GAT GCC ACA G 3′. The average threshold cycle ($C_t$) for each gene was determined from duplicate or triplicate reactions. The target gene expression was normalized to *β-actin* using the difference between their $C_t$ values to generate the $\Delta C_t$. To compare the effects of *Ifngr1* or *Stat1* gene knockout and LPS treatment on DCs, WT immature DCs were set as the reference. The other groups were compared to give the $\Delta\Delta C_t$ value. The fold change of target gene expression is given by the formula $2^{-\Delta\Delta Ct}$.

*Western blot.*

Proteins were extracted from cultured cells for immunoblotting using a modified RIPA buffer. Total protein lysates (25-40 μg/ml per lane) were separated by 4–12% polyacrylamide gel electrophoresis (Bio-Rad). After transfer, the blots were incubated with antibodies against LC3II (Cell signaling) and β-actin (Sigma) and then visualized using SuperSignal Chemiluminescent Substrate (Pierce).

*Statistical analysis.*

Survival data are presented as Kaplan-Meier survival curves, and differences between groups were analyzed by the log-rank test using GraphPad Prism version 9.4.1 (GraphPad Software). The Shapiro-Wilk test was used to assess data normality. Differences between group mean values were tested using a two-tailed Student's *t*-test or the Mann-Whitney *U*-test for non-parametric data. A p-value of $<0.05$ was considered significant. When more than two groups were compared, a 2-way ANOVA test was utilized with Dunnett's correction for multiple comparisons with a control group. Sidak's correction was used for comparing groups of means.

*Study Approval.* The Columbia University IACUC approved all animal procedures.

**Author contributions:**

CL and HHM contributed equally and shared first authorship. They designed and conducted the experiments, generated the manuscript figures, and wrote the manuscript. CL wrote the initial draft and is therefore listed first, LS, HW, LW, SL, and KH conducted or assisted with performing experiments and analyzing the data. AS and SL reviewed the histology. SSP helped with the statistical analysis of the data. YYG and SL contributed to the design of the experiments, analysis of the data, and writing of the manuscript. MYM designed and supervised the experiments and wrote the manuscript.

**Acknowledgments**

This work was supported by NIH grants R01HL093716, RO1EB025221 (MYM) and R01CA175319 (SL), R01CA252756-01A1 (SL and MYM) and by the Pittsburgh Foundation (Grant 2007-M0028, MYM). Research reported in this publication was performed in the CCTI Flow Cytometry Core, supported in part by the Office of the Director, National Institutes of Health, under awards S10RR027050, S10OD020056, S10OD030282, and P30CA013696. The content is solely the responsibility of the authors and does not necessarily represent the official views of the National Institutes of Health. We thank Drs. Ran Reshef, Charles Drake, and Remi Creusot for critical reading of the manuscript and helpful discussions.

**References:**

1. Billiau A, and Matthys P. Interferon-gamma: a historical perspective. *Cytokine Growth Factor Rev.* 2009;20(2):97-113.
2. Schroder K, Hertzog PJ, Ravasi T, and Hume DA. Interferon-gamma: an overview of signals, mechanisms and functions. *J Leukoc Biol.* 2004;75(2):163-89.
3. Hu X, and Ivashkiv LB. Cross-regulation of signaling pathways by interferon-gamma: implications for immune responses and autoimmune diseases. *Immunity.* 2009;31(4):539-50.
4. Schulz EG, Mariani L, Radbruch A, and Hofer T. Sequential polarization and imprinting of type 1 T helper lymphocytes by interferon-gamma and interleukin-12. *Immunity.* 2009;30(5):673-83.

5. Mills KH. TLR-dependent T cell activation in autoimmunity. *Nat Rev Immunol.* 2011;11(12):807-22.
6. Yi T, Chen Y, Wang L, Du G, Huang D, Zhao D, et al. Reciprocal differentiation and tissue-specific pathogenesis of Th1, Th2, and Th17 cells in graft-versus-host disease. *Blood.* 2009;114(14):3101-12.
7. Skoglund C, and Scheynius A. Effects of interferon-gamma treatment on the cutaneous DTH reaction in rats. *Arch Dermatol Res.* 1990;282(5):318-24.
8. Lu Y, and Waller EK. Dichotomous role of interferon-gamma in allogeneic bone marrow transplant. *Biol Blood Marrow Transplant.* 2009;15(11):1347-53.
9. Wang H, and Yang YG. The complex and central role of interferon-gamma in graft-versus-host disease and graft-versus-tumor activity. *Immunol Rev.* 2014;258(1):30-44.
10. Robb RJ, and Hill GR. The interferon-dependent orchestration of innate and adaptive immunity after transplantation. *Blood.* 2012;119(23):5351-8.
11. Horwitz MS, Evans CF, McGavern DB, Rodriguez M, and Oldstone MB. Primary demyelination in transgenic mice expressing interferon-gamma. *Nat Med.* 1997;3(9):1037-41.
12. Vermeire K, Heremans H, Vandeputte M, Huang S, Billiau A, and Matthys P. Accelerated collagen-induced arthritis in IFN-gamma receptor-deficient mice. *J Immunol.* 1997;158(11):5507-13.
13. Takashima S, Martin ML, Jansen SA, Fu Y, Bos J, Chandra D, et al. T cell-derived interferon-gamma programs stem cell death in immune-mediated intestinal damage. *Sci Immunol.* 2019;4(42).
14. Burman AC, Banovic T, Kuns RD, Clouston AD, Stanley AC, Morris ES, et al. IFNgamma differentially controls the development of idiopathic pneumonia syndrome and GVHD of the gastrointestinal tract. *Blood.* 2007;110(3):1064-72.
15. Choi J, Ziga ED, Ritchey J, Collins L, Prior JL, Cooper ML, et al. IFNgammaR signaling mediates alloreactive T-cell trafficking and GVHD. *Blood.* 2012;120(19):4093-103.
16. Choi J, Cooper ML, Staser K, Ashami K, Vij KR, Wang B, et al. Baricitinib-induced blockade of interferon gamma receptor and interleukin-6 receptor for the prevention and treatment of graft-versus-host disease. *Leukemia.* 2018;32(11):2483-94.
17. Ma H, Lu C, Ziegler J, Liu A, Sepulveda A, Okada H, et al. Absence of Stat1 in donor CD4(+) T cells promotes the expansion of Tregs and reduces graft-versus-host disease in mice. *J Clin Invest.* 2011;121(7):2554-69.
18. Spoerl S, Mathew NR, Bscheider M, Schmitt-Graeff A, Chen S, Mueller T, et al. Activity of therapeutic JAK 1/2 blockade in graft-versus-host disease. *Blood.* 2014;123(24):3832-42.
19. Assal A, and Mapara MY. Janus Kinase Inhibitors and Cell Therapy. *Front Immunol.* 2021;12:740847.
20. Dendrou CA, Fugger L, and Friese MA. Immunopathology of multiple sclerosis. *Nat Rev Immunol.* 2015;15(9):545-58.
21. Arellano G, Ottum PA, Reyes LI, Burgos PI, and Naves R. Stage-Specific Role of Interferon-Gamma in Experimental Autoimmune Encephalomyelitis and Multiple Sclerosis. *Front Immunol.* 2015;6:492.
22. Willenborg DO, Fordham S, Bernard CC, Cowden WB, and Ramshaw IA. IFN-gamma plays a critical down-regulatory role in the induction and effector phase of myelin oligodendrocyte glycoprotein-induced autoimmune encephalomyelitis. *J Immunol.* 1996;157(8):3223-7.
23. Wang H, Asavaroengchai W, Yeap BY, Wang MG, Wang S, Sykes M, et al. Paradoxical effects of IFN-gamma in graft-versus-host disease reflect promotion of lymphohematopoietic graft-versus-host reactions and inhibition of epithelial tissue injury. *Blood.* 2009;113(15):3612-9.
24. Mauermann N, Burian J, von Garnier C, Dirnhofer S, Germano D, Schuett C, et al. Interferon-gamma regulates idiopathic pneumonia syndrome, a Th17+CD4+ T-cell-mediated graft-versus-host disease. *Am J Respir Crit Care Med.* 2008;178(4):379-88.
25. Delisle JS, Gaboury L, Belanger MP, Tasse E, Yagita H, and Perreault C. Graft-versus-host disease causes failure of donor hematopoiesis and lymphopoiesis in interferon-gamma receptor-deficient hosts. *Blood.* 2008;112(5):2111-9.
26. Feuerer M, Eulenburg K, Loddenkemper C, Hamann A, and Huehn J. Self-limitation of Th1-mediated inflammation by IFN-gamma. *J Immunol.* 2006;176(5):2857-63.
27. Chawla-Sarkar M, Lindner DJ, Liu YF, Williams BR, Sen GC, Silverman RH, et al. Apoptosis and interferons: role of interferon-stimulated genes as mediators of apoptosis. *Apoptosis.* 2003;8(3):237-49.
28. Wang Z, Hong J, Sun W, Xu G, Li N, Chen X, et al. Role of IFN-gamma in induction of Foxp3 and conversion of CD4+ CD25- T cells to CD4+ Tregs. *J Clin Invest.* 2006;116(9):2434-41.

29. Blazar BR, Carreno BM, Panoskaltsis-Mortari A, Carter L, Iwai Y, Yagita H, et al. Blockade of programmed death-1 engagement accelerates graft-versus-host disease lethality by an IFN-gamma-dependent mechanism. *J Immunol.* 2003;171(3):1272-7.
30. Whitley K, Hoebe K, and Beutler B. Phenotypic Mutation 'poison. https://mutagenetix.utsouthwestern.edu/phenotypic/phenotypic_rec.cfm?pk=285.
31. Koyama M, Kuns RD, Olver SD, Raffelt NC, Wilson YA, Don AL, et al. Recipient nonhematopoietic antigen-presenting cells are sufficient to induce lethal acute graft-versus-host disease. *Nat Med.* 2012;18(1):135-42.
32. Cooke KR, Gerbitz A, Crawford JM, Teshima T, Hill GR, Tesolin A, et al. LPS antagonism reduces graft-versus-host disease and preserves graft-versus-leukemia activity after experimental bone marrow transplantation. *J Clin Invest.* 2001;107(12):1581-9.
33. Heine A, Held SA, Daecke SN, Wallner S, Yajnanarayana SP, Kurts C, et al. The JAK-inhibitor ruxolitinib impairs dendritic cell function *in vitro* and *in vivo*. *Blood.* 2013;122(7):1192-202.
34. Blazar BR, Murphy WJ, and Abedi M. Advances in graft-versus-host disease biology and therapy. *Nat Rev Immunol.* 2012;12(6):443-58.
35. Rudensky A, Rath S, Preston-Hurlburt P, Murphy DB, and Janeway CA, Jr. On the complexity of self. *Nature.* 1991;353(6345):660-2.
36. Huang S, Hendriks W, Althage A, Hemmi S, Bluethmann H, Kamijo R, et al. Immune response in mice that lack the interferon-gamma receptor. *Science.* 1993;259(5102):1742-5.
37. Kamijo R, Le J, Shapiro D, Havell EA, Huang S, Aguet M, et al. Mice that lack the interferon-gamma receptor have profoundly altered responses to infection with Bacillus Calmette-Guerin and subsequent challenge with lipopolysaccharide. *J Exp Med.* 1993;178(4):1435-40.
38. Durbin JE, Hackenmiller R, Simon MC, and Levy DE. Targeted disruption of the mouse Stat1 gene results in compromised innate immunity to viral disease. *Cell.* 1996;84(3):443-50.
39. Meraz MA, White JM, Sheehan KC, Bach EA, Rodig SJ, Dighe AS, et al. Targeted disruption of the Stat1 gene in mice reveals unexpected physiologic specificity in the JAK-STAT signaling pathway. *Cell.* 1996;84(3):431-42.
40. Neefjes J, Jongsma ML, Paul P, and Bakke O. Towards a systems understanding of MHC class I and MHC class II antigen presentation. *Nat Rev Immunol.* 2011;11(12):823-36.
41. Nakagawa TY, Brissette WH, Lira PD, Griffiths RJ, Petrushova N, Stock J, et al. Impaired invariant chain degradation and antigen presentation and diminished collagen-induced arthritis in cathepsin S null mice. *Immunity.* 1999;10(2):207-17.
42. Morris P, Shaman J, Attaya M, Amaya M, Goodman S, Bergman C, et al. An essential role for HLA-DM in antigen presentation by class II major histocompatibility molecules. *Nature.* 1994;368(6471):551-4.
43. Denzin LK, and Cresswell P. HLA-DM induces CLIP dissociation from MHC class II alpha beta dimers and facilitates peptide loading. *Cell.* 1995;82(1):155-65.
44. van Niel G, Wubbolts R, Ten Broeke T, Buschow SI, Ossendorp FA, Melief CJ, et al. Dendritic cells regulate exposure of MHC class II at their plasma membrane by oligoubiquitination. *Immunity.* 2006;25(6):885-94.
45. De Gassart A, Camosseto V, Thibodeau J, Ceppi M, Catalan N, Pierre P, et al. MHC class II stabilization at the surface of human dendritic cells is the result of maturation-dependent MARCH I down-regulation. *Proc Natl Acad Sci U S A.* 2008;105(9):3491-6.
46. Corcoran K, Jabbour M, Bhagwandin C, Deymier MJ, Theisen DL, and Lybarger L. Ubiquitin-mediated regulation of CD86 protein expression by the ubiquitin ligase membrane-associated RING-CH-1 (MARCH1). *J Biol Chem.* 2011;286(43):37168-80.
47. Turka LA, and Lechler RI. Towards the identification of biomarkers of transplantation tolerance. *Nat Rev Immunol.* 2009;9(7):521-6.
48. Levine B, Mizushima N, and Virgin HW. Autophagy in immunity and inflammation. *Nature.* 2011;469(7330):323-35.
49. Thome R, Bonfanti AP, Rasouli J, Mari ER, Zhang GX, Rostami A, et al. Chloroquine-treated dendritic cells require STAT1 signaling for their tolerogenic activity. *Eur J Immunol.* 2018;48(7):1228-34.
50. Vogel A, Martin K, Soukup K, Halfmann A, Kerndl M, Brunner JS, et al. JAK1 signaling in dendritic cells promotes peripheral tolerance in autoimmunity through PD-L1-mediated regulatory T cell induction. *Cell Rep.* 2022;38(8):110420.

51. Ma HH, Ziegler J, Li C, Sepulveda A, Bedeir A, Grandis J, et al. Sequential activation of inflammatory signaling pathways during graft-versus-host disease (GVHD): early role for STAT1 and STAT3. *Cell Immunol.* 2011;268(1):37-46.
52. Sun K, Hsiao HH, Li M, Ames E, Bouchlaka M, Welniak LA, et al. IFN-gamma receptor-deficient donor T cells mediate protection from graft-versus-host disease and preserve graft-versus-tumor responses after allogeneic bone marrow transplantation. *J Immunol.* 2012;189(4):2033-42.
53. Ellison CA, Fischer JM, HayGlass KT, and Gartner JG. Murine graft-versus-host disease in an F1-hybrid model using IFN-gamma gene knockout donors. *J Immunol.* 1998;161(2):631-40.
54. Brok HP, Heidt PJ, van der Meide PH, Zurcher C, and Vossen JM. Interferon-gamma prevents graft-versus-host disease after allogeneic bone marrow transplantation in mice. *J Immunol.* 1993;151(11):6451-9.
55. Stickel N, Hanke K, Marschner D, Prinz G, Kohler M, Melchinger W, et al. MicroRNA-146a reduces MHC-II expression via targeting JAK/STAT signaling in dendritic cells after stem cell transplantation. *Leukemia.* 2017;31(12):2732-41.
56. Taganov KD, Boldin MP, Chang KJ, and Baltimore D. NF-kappaB-dependent induction of microRNA miR-146, an inhibitor targeted to signaling proteins of innate immune responses. *Proc Natl Acad Sci U S A.* 2006;103(33):12481-6.
57. Fu J, Wu Y, Nguyen H, Heinrichs J, Schutt S, Liu Y, et al. T-bet Promotes Acute Graft-versus-Host Disease by Regulating Recipient Hematopoietic Cells in Mice. *J Immunol.* 2016;196(7):3168-79.
58. Bettelli E, Sullivan B, Szabo SJ, Sobel RA, Glimcher LH, and Kuchroo VK. Loss of T-bet, but not STAT1, prevents the development of experimental autoimmune encephalomyelitis. *J Exp Med.* 2004;200(1):79-87.
59. Schonfelder T, Brandt M, Kossmann S, Knopp T, Munzel T, Walter U, et al. Lack of T-bet reduces monocytic interleukin-12 formation and accelerates thrombus resolution in deep vein thrombosis. *Sci Rep.* 2018;8(1):3013.
60. Lugo-Villarino G, Maldonado-Lopez R, Possemato R, Penaranda C, and Glimcher LH. T-bet is required for optimal production of IFN-gamma and antigen-specific T cell activation by dendritic cells. *Proc Natl Acad Sci U S A.* 2003;100(13):7749-54.
61. Capitini CM, Nasholm NM, Chien CD, Larabee SM, Qin H, Song YK, et al. Absence of STAT1 in donor-derived plasmacytoid dendritic cells results in increased STAT3 and attenuates murine GVHD. *Blood.* 2014;124(12):1976-86.
62. Shao WH, Gamero AM, Zhen Y, Lobue MJ, Priest SO, Albandar HJ, et al. Stat1 Regulates Lupus-like Chronic Graft-versus-Host Disease Severity via Interactions with Stat3. *J Immunol.* 2015;195(9):4136-43.

**Figure 1.**

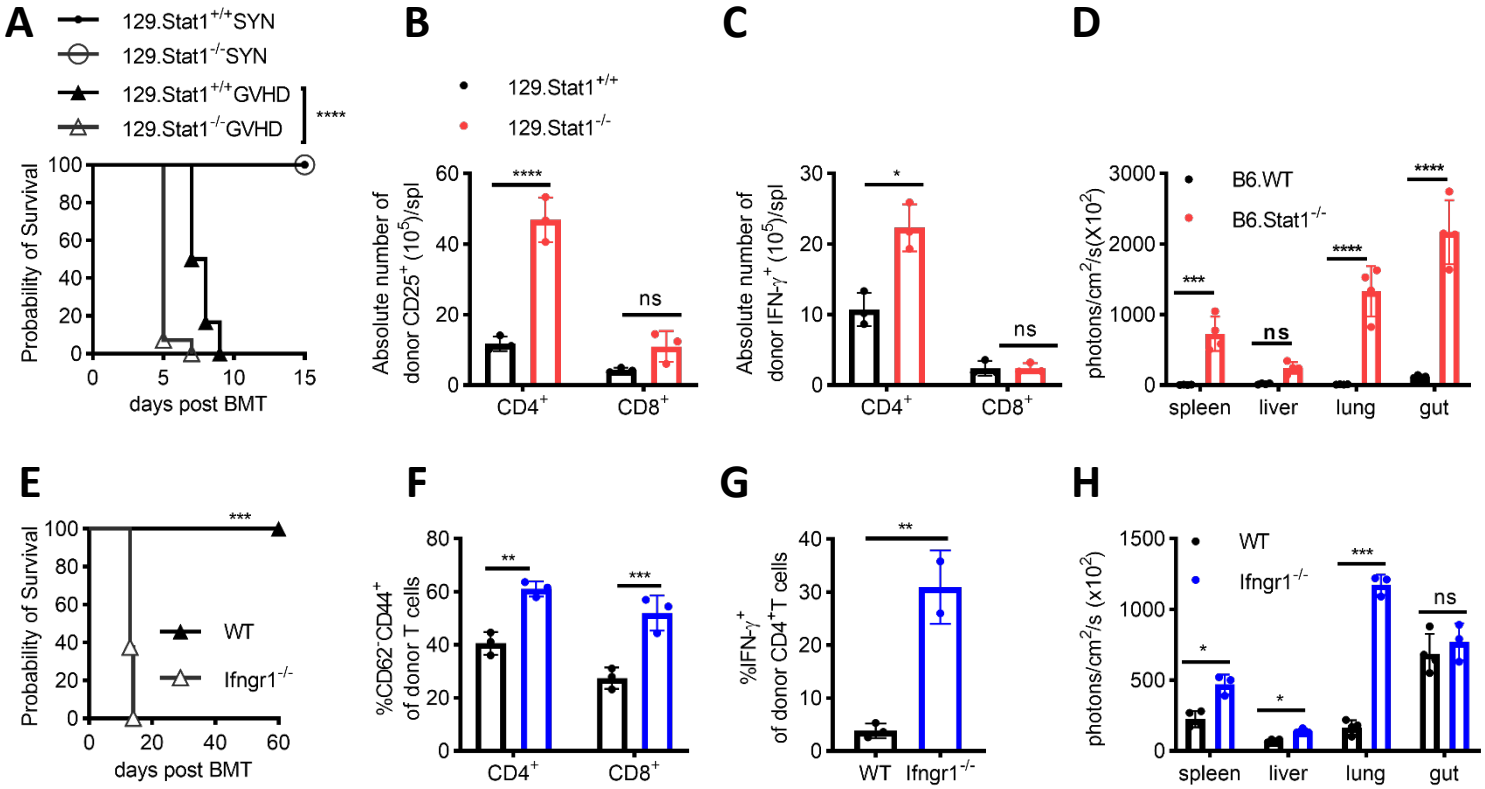
A
129.Stat1+/+SYN
129.Stat1-/-SYN
129.Stat1+/+GVHD
129.Stat1-/-GVHD
****
Probability of Survival
days post BMT
B
129.Stat1+/+
129.Stat1-/-
Absolute number of donor CD25+ (10^5)/spl
CD4+
CD8+
ns
C
Absolute number of donor IFN-γ+ (10^5)/spl
D
B6.WT
B6.Stat1-/-
photons/cm2/s(X10^2)
spleen
liver
lung
gut
E
WT
Ifngr1-/-
F
%CD62-CD44+ of donor T cells
G
%IFN-γ+ of donor CD4+T cells
H
WT
Ifngr1-/-
photons/cm2/s (x10^2)

***Figure 1. Absence of host IFNGR/STAT1 signaling enhances GVHD induction.***

GVHD was induced in the fully MHC-mismatched (BALB/c [$H2^d$] to 129Sv [$H2^b$]) strain combination. **A)** Lethally irradiated (1,044 cGy) 129.$Stat1^{-/-}$ or 129.$Stat1^{+/+}$ mice received $5x10^6$ BMC and $1x10^7$ splenocytes from BALB/c mice; data from 2 similar experiments with 12-14 animals/group; survival data was analyzed by log rank test. **B-C)** CD25 expression (B) and intracellular IFN-γ expression (**C**) on donor ($H2D^d$) $CD4^+$ or $CD8^+$ T cells in the host splenic cells were tested on day +4 post-BMT; Representative results of one of 2 independent experiments with 3-4 animals/group are shown. **D)** The *in vivo* expansion of alloreactive donor BALB/c-luc T cells and target organ infiltration in B6.WT or *Stat1*$^{-/-}$ recipients was assessed by BLI on day+6 post-BMT. Representative results of one of 3 independent experiments with 3-4 animals per group are shown. **E-H)** Fully MHC-mismatched GVHD induction following lethal irradiation in B6 (WT, n=5) vs. *B6.Ifngr1*$^{-/-}$ recipients (*Ifngr1*$^{-/-}$, n=8) using $1x10^7$ splenocytes and $5x10^6$ BMCs from BALB/c-luc mice. Survival data was analyzed by log rank test. Activation of the donor ($H2^{d+}$) $CD4^+$, $CD8^+$, lymphocytes, (**F**) and intracellular IFN-γ staining in donor-derived $CD4^+$ T cells (**G**) was tested on day +4 post-BMT. (**H**) Recipient animals were monitored for infiltration and expansion of BALB/c-luc lymphocytes on day +7 post-BMT using BLI. Representative results of one of 2 independent experiments with 3-4 animals/group are shown. Bar graphs represent the mean ± SEM; p values were calculated by 2-way ANOVA with Sidak correction except for **G,** where a student t test was used. * $p<0.05$, ** $p<0.01$, *** $p<0.001$, **** $p<0.0001$.

**Figure 2.**

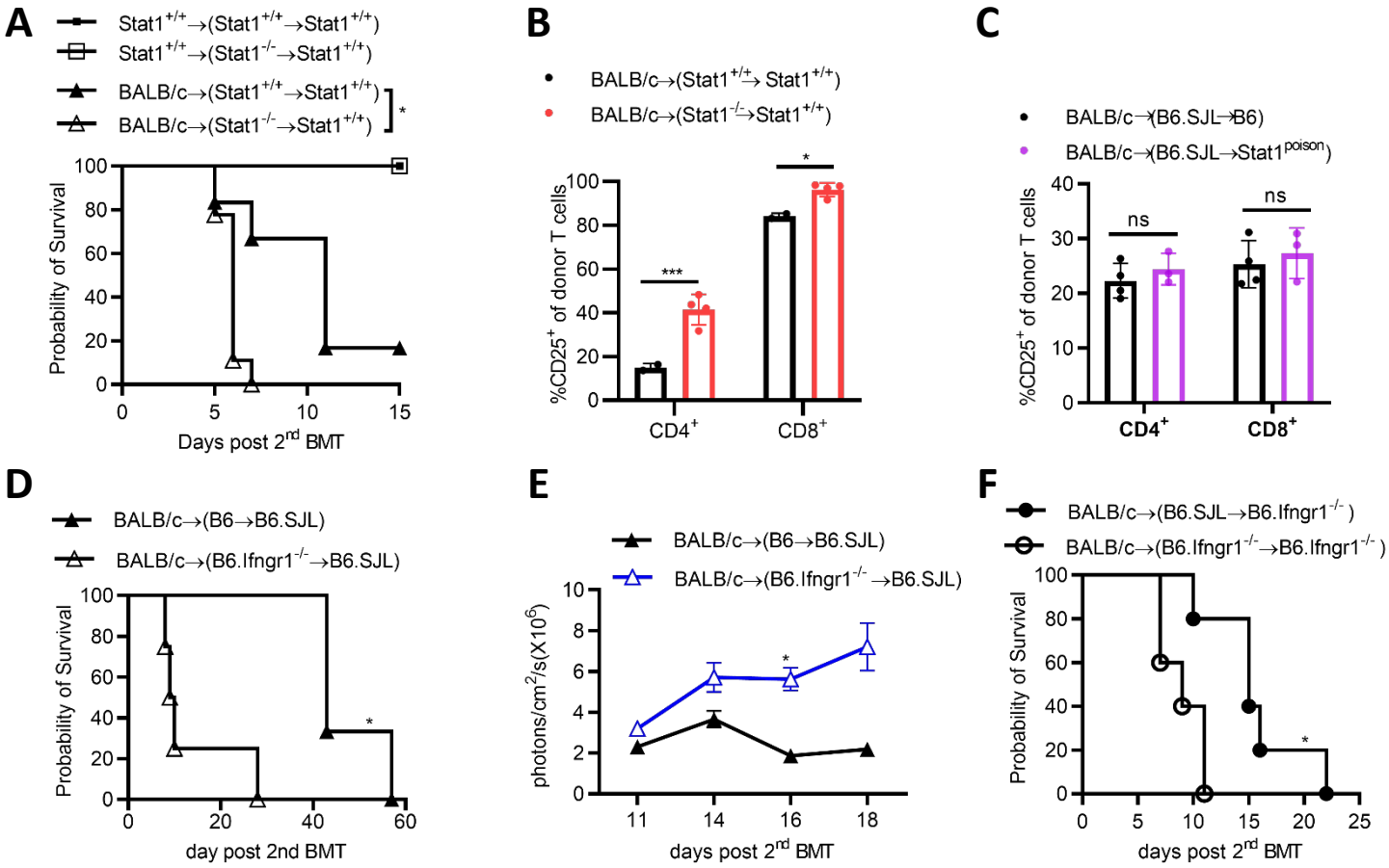
A
Stat1+/+→(Stat1+/+→Stat1+/+)
Stat1+/+→(Stat1-/-→Stat1+/+)
BALB/c→(Stat1+/+→Stat1+/+)
BALB/c→(Stat1-/-→Stat1+/+)
*
Probability of Survival
Days post 2nd BMT
B
BALB/c→(Stat1+/+→ Stat1+/+)
BALB/c→(Stat1-/-→Stat1+/+)
%CD25+ of donor T cells
***
*
CD4+
CD8+
C
BALB/c→(B6.SJL→B6)
BALB/c→(B6.SJL→Stat1poison)
%CD25+ of donor T cells
ns
ns
CD4+
CD8+
D
BALB/c→(B6→B6.SJL)
BALB/c→(B6.Ifngr1-/-→B6.SJL)
Probability of Survival
*
day post 2nd BMT
E
BALB/c→(B6→B6.SJL)
BALB/c→(B6.Ifngr1-/- →B6.SJL)
photons/cm2/s(X10^6)
*
days post 2nd BMT
F
BALB/c→(B6.SJL→B6.Ifngr1-/- )
BALB/c→(B6.Ifngr1-/-→B6.Ifngr1-/- )
Probability of Survival
*
days post 2nd BMT

***Figure 2. Contribution of hematopoietic versus non-hematopoietic IFNGR/STAT1 deficiency to the development of GVHD.***

**A-**B) GVHD was induced in radiation chimeras with STAT1 deficiency in the hematopoietic compartment (*129.Stat1*$^{-/-}$→*129.Stat1*$^{+/+}$). The data are representative of two similar experiments with 9-12 mice/group. (**A** MST 6 days vs. 11 days, log-rank test p=0.02). CD25 expression on donor (H-2$^{d}$) CD4 and CD8 T cells was tested on day +6 post-BMT (**B**). **C**) Donor lymphocyte activation was assessed in chimeric mice with STAT1 deficiency restricted to non-hematopoietic cells using *B6.Stat1*$^{Poison}$ mice. Lethally irradiated (1,075 cGy) *B6.Stat1*$^{Poison}$ mice or B6 wild-type mice received 5x10$^{6}$ BMCs from B6.SJL syngeneic wild-type mice. Four months after the first transplantation, chimeras were irradiated (1,075 cGy) and injected with 5x10$^{6}$ BMCs and 1x10$^{7}$ splenocytes from BALB/c mice. CD25 expression on donor (H-2$^{d}$) CD4$^{+}$ and CD8$^{+}$ T cells was tested on day +7 post-BMT, n=5 mice/group. **D-F)** GVHD induction in radiation chimeras with IFNGR deficiency in the hematopoietic (*B6.Ifngr1*$^{-/-}$→B6.SJL **D, E**) and non-hematopoietic compartment (B6.SJL→ *B6.Ifngr1*$^{-/-}$ **F**). **D**) Survival analysis was performed using a log-rank test (MST 9.5 days vs. 43 days, * log-rank test p<0.05, n=3-6 mice/group). **E**) *In vivo* expansion of BALB/c-luc lymphocytes in recipient animals was monitored *in vivo* using BLI at the indicated days after the second transplantation. **F**) Survival curve following GVHD induction in *Ifngr1*$^{-/-}$→ Ifngr1$^{-/-}$chimeras with BALB/c spleen cells (MST 15 days vs. 9 days, log-rank test p<0.05, n=5-6 mice/group). Bar graphs represent the mean ± SEM; p values were calculated by 2way ANOVA with Sidak correction * p<0.05, ** p<0.01.

**Figure 3.**

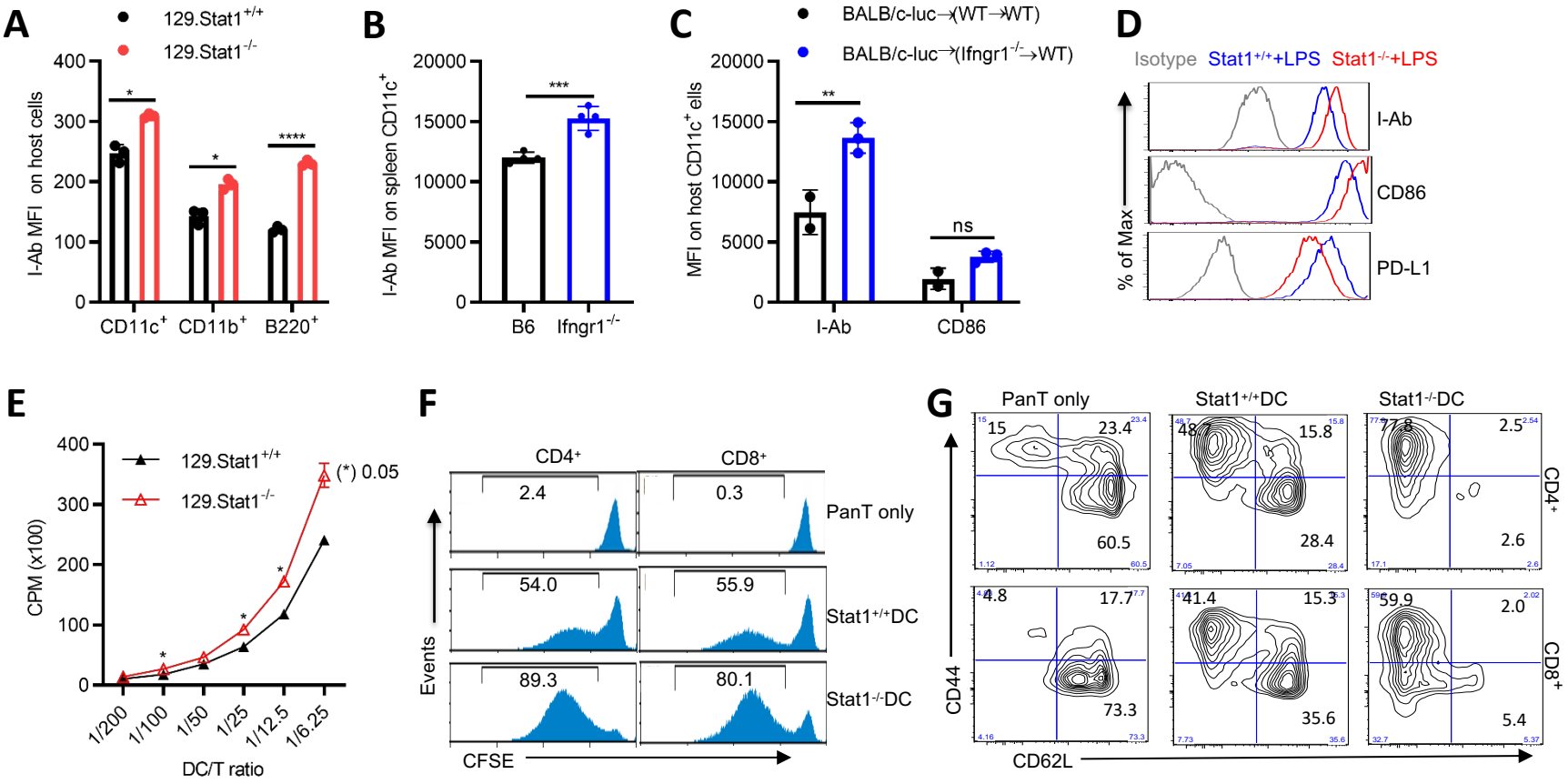
A
129.Stat1+/+
129.Stat1-/-
I-Ab MFI on host cells
CD11c+
CD11b+
B220+
B
I-Ab MFI on spleen CD11c+
B6
Ifngr1-/-
C
BALB/c-luc→(WT→WT)
BALB/c-luc→(Ifngr1-/-→WT)
MFI on host CD11c+ ells
I-Ab
CD86
ns
D
Isotype
Stat1+/+LPS
Stat1-/-LPS
% of Max
I-Ab
CD86
PD-L1
E
129.Stat1+/+
129.Stat1-/-
(*) 0.05
CPM (x100)
DC/T ratio
1/200
1/100
1/50
1/25
1/12.5
1/6.25
F
CD4+
CD8+
2.4
0.3
PanT only
54.0
55.9
Stat1+/+DC
89.3
80.1
Stat1-/-DC
Events
CFSE
G
PanT only
Stat1+/+DC
Stat1-/-DC
15
23.4
60.5
48
15.8
28.4
2.5
2.6
4.8
17.7
73.3
41.4
15.3
35.6
59.9
2.0
5.4
CD4+
CD8+
CD44
CD62L

***Figure 3. Absence of IFNGR/STAT1 promotes allostimulatory capacity in DCs.***

**A**) On day+1 post-BMT different APC populations were analyzed from recipient animals following induction of GVHD using a fully MHC-mismatched (BALB/c [$H2^d$] to 129Sv [$H2^b$]) strain combination. MHC II expression on recipient spleen $H2^{b+}$ $CD11c^+$, $CD11b^+$, and $B220^+$ cells from recipient *129.Stat1*$^{+/+}$ and *129. Stat1*$^{-/-}$ animals. One representative experiment from three is shown with 3 animals/group. **B**) GVHD was induced in the fully MHC-mismatched BALB/c [$H2^d$] to B6 [$H2^b$]) strain combination in B6 wildtype or *B6.Ifngr1*$^{-/-}$ mice. I-$A^b$ expression on recipient splenic $CD11c^+$ cells was studied on day +1 post-BMT. One representative experiment from two is shown with 3-4 animals/group **C**) I-Ab and CD86 expression on the recipient $CD11c^+$ cells in *Ifngr1*$^{-/-}$→B6.SJL chimeric recipients were compared with that in the B6→B6.SJL counterparts two days following the second transplantation of BALB/c TCD-BMC and BALB/c-Luc splenocytes. One representative experiment from two is shown with 2-3 animals per group **D**) I-Ab, CD86, and PD-L1 expression measured on $CD11c^+$ BMDCs from *Stat1*$^{+/+}$ or *Stat1*$^{-/-}$ mice cultured in RPMI 1640 medium containing 10% FCS and GM-CSF (20 ng/ml) for six days and matured in 100 ng/ml LPS for an additional 48 h. One representative from more than 3 independent experiments is shown. **E-G)** Proliferation and activation of CFSE-labeled alloreactive pan-T cells isolated from BALB/c splenocytes stimulated with LPS-matured *Stat1*$^{+/+}$ or *Stat1*$^{-/-}$ BMDCs. Freshly isolated pan-T cells from BALB/c mice cells were stimulated with LPS-matured *Stat1*$^{+/+}$ or *Stat1*$^{-/-}$ BMDCs at a DC/Responder ratio of 1:5 for five days. The proliferation of responder cells was assessed by $^3$H-incorporation presented as CPM ratio compared to unstimulated responder cells (E) or by the CFSE dilution presented as the percentage of $CFSE^{lo}$ population (**F**), and the T cell activation was measured by CD44 and CD62L expression in responder $CD4^+$ or $CD8^+$ T cells (**G**). One representative from three independent experiments is shown. Bar graphs represent the mean ± SEM; p values were calculated by 2-way ANOVA with Sidak correction * $p<0.05$, ** $p<0.01$.

**Figure 4.**

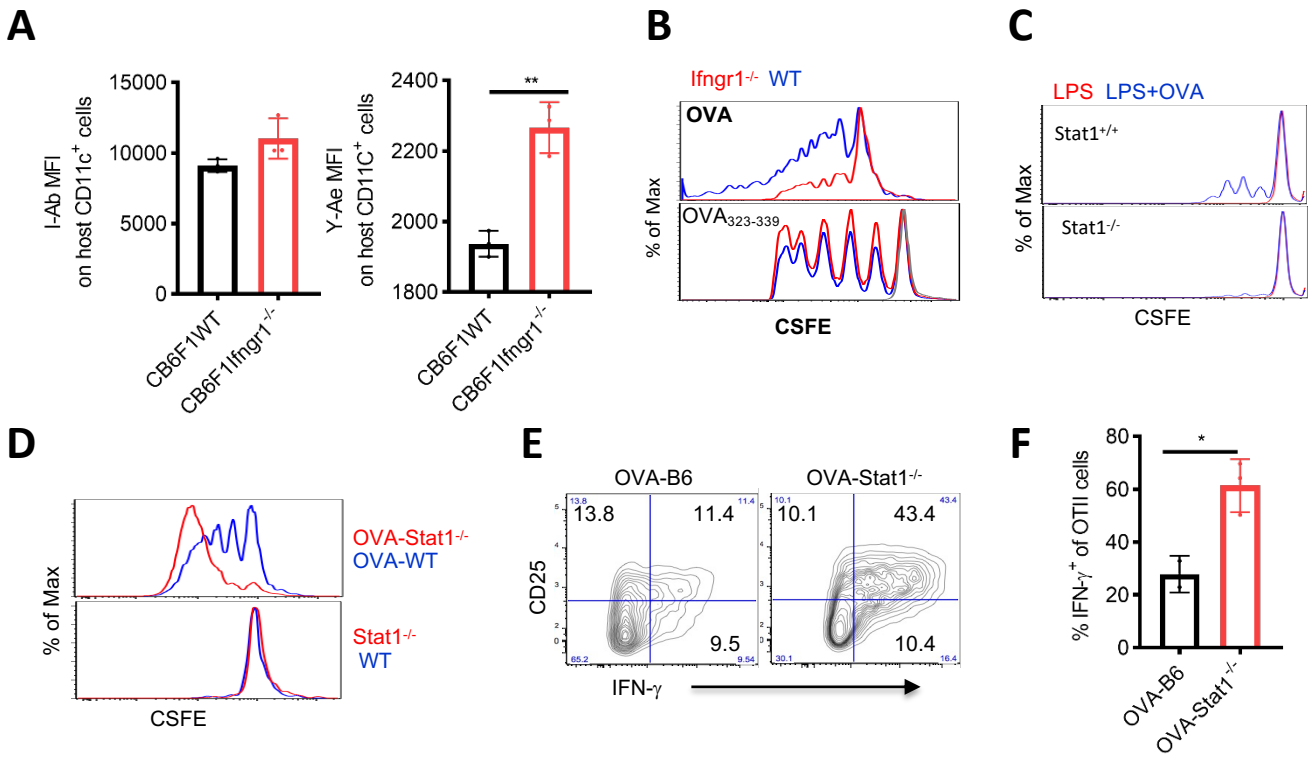
A
I-Ab MFI on host CD11c+ cells
15000
10000
5000
0
CB6F1WT
CB6F1Ifngr1-/-
Y-Ae MFI on host CD11C+ cells
2400
2200
2000
1800
**
B
Ifngr1-/- WT
OVA
OVA323-339
% of Max
CSFE
C
LPS LPS+OVA
Stat1+/+
Stat1-/-
% of Max
CSFE
D
% of Max
OVA-Stat1-/-
OVA-WT
Stat1-/-
WT
CSFE
E
OVA-B6
OVA-Stat1-/-
13.8
11.4
9.5
10.1
43.4
10.4
CD25
IFN-γ
F
% IFN-γ+ of OTII cells
80
60
40
20
0
*
OVA-B6
OVA-Stat1-/-

***Figure 4. Absence of IFNGR/STAT1 signaling leads to enhanced endogenous and compromised exogenous antigen presentation.***

**A)** GVH was induced in the parent-into-F1 mouse model without irradiation. CB6F1 [$H2^{bd}$]) wild-type or *Ifngr1*$^{-/-}$ mice received $5x10^6$ BMCs and $2.5\text{-}3x10^7$ splenocytes from B6.SJL mice. The data are representative of two similar experiments with five animals/group. Increased I-Ab expression and recipient-derived endogenous Ea52-68 peptide presentation (tested by Y-Ae staining) on $CD11c^+$ cells on day +2 post-BMT. **B-C)** OT-II T cell proliferation was determined by CFSE dilution in response to 3 days of stimulation with 0.5% PFA fixed *B6.Ifngr1* $^{-/-}$ or Stat1$^{-/-}$ BMDCs. BMDCs were incubated for 1hr with Ovalbumin (100ng/ml), then overnight in the presence of LPS. For $OVA_{323\text{-}339}$ peptide loading, BMDCs were matured with LPS, fixed with 0.5%PFA, and then pulsed with 100ng/ml $OVA_{323\text{-}339}$ peptides for 0.5hr. **D**) OT-II proliferation in response to 3 days of stimulation with WT act-mOVA (OVA-B6) or *Stat1*$^{-/-}$ x act-mOVA (OVA-*Stat1*$^{-/-}$) BMDCs after LPS overnight maturation. WT and *Stat1*$^{-/-}$ BMDCs without constitutive OVA expression were used as controls. **E**) OVA-B6 or OVA-*Stat1*$^{-/-}$ were lethally irradiated (1075rad) and received $3x10^6$ splenocytes from OTII mice. CD25 and IFN-γ expression were detected in OT-II cells five days after injection, n=2-3 mice/group. Bar graphs (A, E) represent the mean ± SEM; p values were calculated by 2-tailed student t-test * $p<0.05$, ** $p<0.01$.

**Figure 5.**

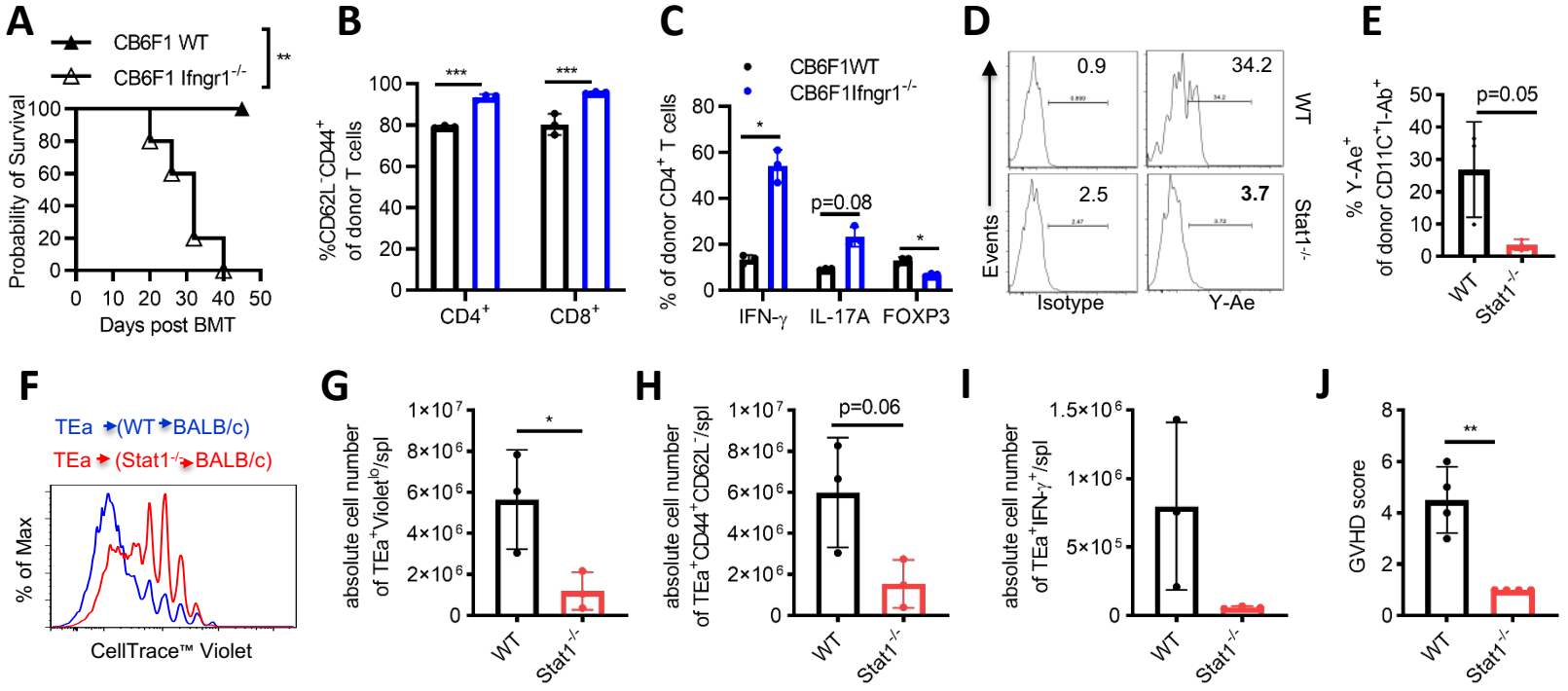
A
CB6F1 WT
CB6F1 Ifngr1-/-
**
Probability of Survival
Days post BMT
B
***
***
%CD62L-CD44+ of donor T cells
CD4+
CD8+
C
CB6F1WT
CB6F1Ifngr1-/-
*
p=0.08
*
% of donor CD4+ T cells
IFN-γ
IL-17A
FOXP3
D
0.9
34.2
2.5
3.7
WT
Stat1-/-
Events
Isotype
Y-Ae
E
p=0.05
% Y-Ae+ of donor CD11C+I-Ab+
WT
Stat1-/-
F
TEa →(WT→BALB/c)
TEa →(Stat1-/-→BALB/c)
% of Max
CellTrace™ Violet
G
*
absolute cell number of TEa+Violetlo/spl
WT
Stat1-/-
H
p=0.06
absolute cell number of TEa+CD44+CD62L-/spl
WT
Stat1-/-
I
absolute cell number of TEa+IFN-γ+/spl
WT
Stat1-/-
J
**
GVHD score
WT
Stat1-/-

***Figure 5. APCs with deficient IFNGR/STAT1 signaling exhibit increased direct and compromised indirect antigen presentation.***

**A**) GVHD was induced in the P →F1 (B6.SJL[$H2^b$] →CB6F1 [$H2^{bxd}$]) mouse model using wild-type or *Ifngr1*$^{-/-}$ recipients. GVHD mortality was monitored. *Ifngr1*$^{-/-}$ F1 recipient mice exhibited significantly increased GVHD mortality (MST 32 days vs. not reached, log-rank test ** $p<0.01$, n=5 mice/group). **B-C)** spleen T cell activation was determined by the percentage of $CD62L^-CD44^+$ in donor T cells, and differentiation (Th1, Th17, and $T_{reg}$) assessed by IFN-γ, IL17A, and FOXP3 expression in donor $CD4^+$T cells on day +7 post-BMT, n=3 mice/group. **D, E)** Donor-derived $CD11c^+$ cells were assessed d+18 post-transplant for MHC II ($I\text{-}A^b$) and associated Ea52-68 peptide presentation (Y-Ae expression) following fully MHC-mismatched BMT in BALB/c mice receiving $5x10^6$ TCD BMCs from either wild-type B6 or *Stat1*$^{-/-}$ mice after 800 rad irradiation (n=3 mice/group). **F-J)** *In vivo* proliferation of TEa-TCR-transgenic T cells specific for Ea52-68 peptide presented by $I\text{-}A^b$. Three weeks post-transplant, $5x10^6$ CellTrace™ Violet-labeled pan T cells from TEa-TCR-transgenic mice were administered i.v. to B6.WT→BALB/c or B6.*Stat1*$^{-/-}$→BALB/c chimeras. Proliferation was determined by CellTrace™ Violet dilution (F, G), activation (H), and Th1 differentiation (I) of antigen-specific TEa TCR+ donor T cells ($CD4^+Va2^+Vb6^+$) on day +5 post-donor lymphocyte infusion (DLI) (n=3 mice/group). J) Clinical GVHD scores were recorded at day+7 post-DLI of TEa-TCR-transgenic T cells (n=4 mice/group). Bar graphs represent the mean ± SEM, p values were calculated 2-way ANOVA with Sidak correction (B, C) and by 2-tailed t test (E, G-J) * $p<0.05$, ** $p<0.01$.

**Figure 6.**

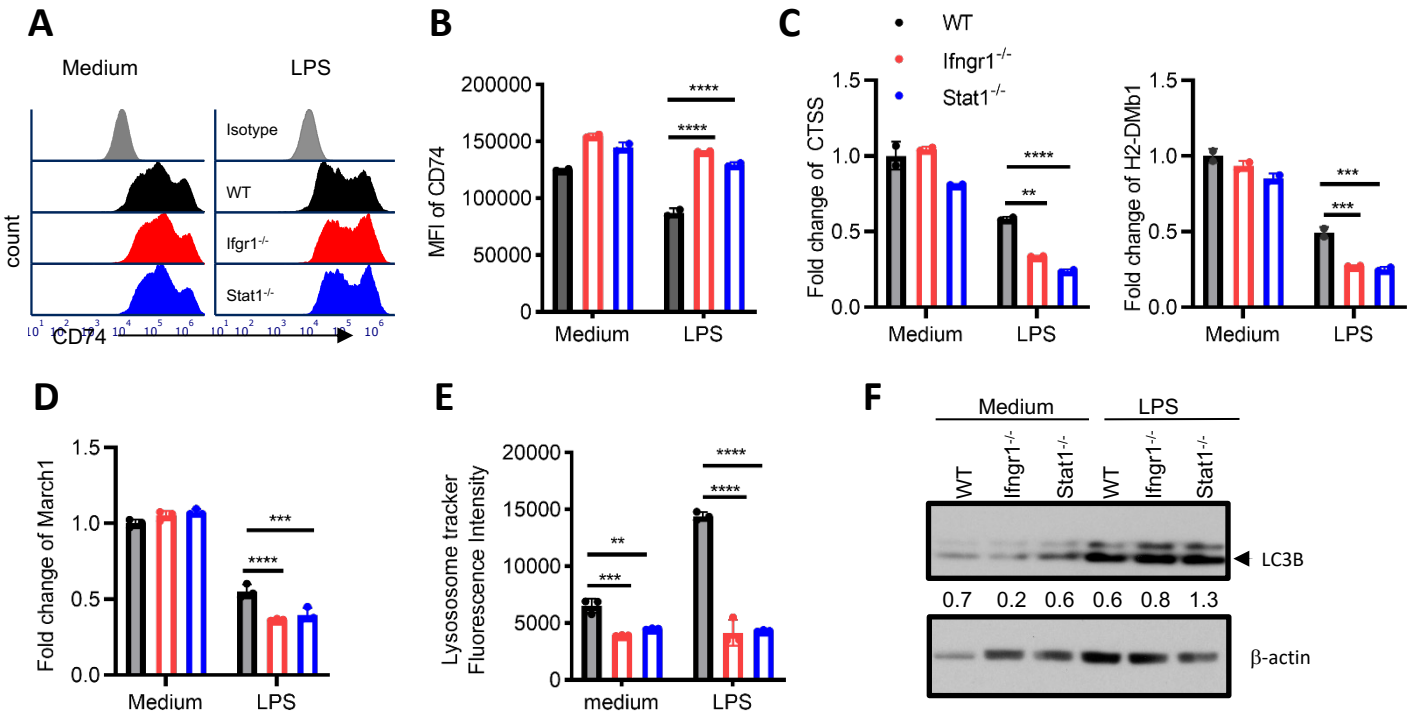
A
Medium
LPS
Isotype
WT
Ifgr1-/-
Stat1-/-
count
CD74
B
MFI of CD74
200000
150000
100000
50000
0
****
****
Medium
LPS
C
WT
Ifngr1-/-
Stat1-/-
Fold change of CTSS
1.5
1.0
0.5
0.0
****
**
Medium
LPS
Fold change of H2-DMb1
1.5
1.0
0.5
0.0
***
***
Medium
LPS
D
Fold change of March1
1.5
1.0
0.5
0.0
***
****
Medium
LPS
E
Lysosome tracker Fluorescence Intensity
20000
15000
10000
5000
0
**
***
****
****
medium
LPS
F
Medium
LPS
WT
Ifngr1-/-
Stat1-/-
WT
Ifngr1-/-
Stat1-/-
LC3B
0.7
0.2
0.6
0.6
0.8
1.3
β-actin

**Figure 6. BMDCs with IFNGR/STAT1 deficiency exhibit impaired peptide exchange and reduced turnover of surface MHC II upon LPS maturation.**

**A, B)** CD74 expression on $CD11c^+$ BMDCs from B6 WT (black), *B6.Ifngr1*$^{-/-}$ (red) and *Stat1*$^{-/-}$ (blue) mice after LPS 48hr, isotype control was labeled with a gray histogram. **C, D)** Quantitative RT-PCR analysis of Cathepsin S (*Ctss*), *H2-DMb1*, and *March1* mRNA expression in $CD11c^+$ BMDCs incubated in the presence or absence of LPS for 4 hr. **E)** Quantitation of lysosome tracker staining of immature or LPS maturated BMDCs from WT, *Ifngr1*$^{-/-}$ or *Stat1*$^{-/-}$ mice by flow cytometry. **F)** LC3B expression in WT, *Ifngr1*$^{-/-}$ and *Stat1*$^{-/-}$ BMDCs after 48 hr LPS maturation was tested by Western blotting, semi-quantified by Image J. Bar graphs represent the mean ± SEM. Results were analyzed by 2-way ANOVA testing and Dunnett's correction for multiple comparisons versus the wildtype control. * $p<0.05$, ** $p<0.01$, *** $p<0.001$.